Bedrock geology of Truitt Creek map area (NTS 105L/1) and tectonic implications for the northern Canadian Cordillera, central Yukon Territory

by

Kaesy Gladwin
B.Sc., Acadia University, 2001

A thesis submitted in partial fulfillment of the
requirements for the degree of

MASTER OF SCIENCE

in the School of Earth and Ocean Sciences

© Kaesy Gladwin, 2003
University of Victoria

All rights reserved. This thesis may not be reproduced in whole or in part, by photocopy or other means, without the permission of the author.

Supervisor: Dr. Stephen T. Johnston

ABSTRACT

In southern central Yukon Territory, Canada, a northwest-trending 267 Ma ophiolitic assemblage defines the Tummel fault zone (TFZ), which juxtaposes Paleozoic miogeoclinal strata of Cassiar terrane with metavolcanic and metasedimentary rocks of Yukon-Tanana terrane. Basalt, greenstone, and chert occur in the TFZ and are correlated with Slide Mountain terrane. Northeast of the TFZ, pelitic and semipelitic rocks of the Kechika Group are overlain by carbonate of the Askin Group in Cassiar terrane. Southwest of the TFZ, Yukon-Tanana terrane comprises Devonian-Mississippian quartzofeldspathic basement (the Snowcap Complex) overlain by Mississippian clastic and arc-derived rocks of the Drury, Pelmac, and Little Salmon formations.

The ca. 105 Ma Glenlyon Batholith and its satellite plutons intrude Cassiar terrane and the TFZ, imposing a contact metamorphic aureole that overprints earlier metamorphic features in rocks of Cassiar and Yukon-Tanana terranes and the TFZ, and indicates pre-105 Ma juxtaposition of these three tectonic assemblages.

TABLE OF CONTENTS

ABSTRACT....ii

TABLE OF CONTENTS....iii

LIST OF TABLES....iv

LIST OF FIGURES....iv

ACKNOWLEDGEMENTS....vii

CHAPTER 1: INTRODUCTION

REGIONAL GEOLOGY....1
GEOLOGY OF THE STUDY AREA....2
CARMACKS GROUP PALEOMAGNETIC DATA....3
STUDY OVERVIEW....4
METHODOLOGY....5
REFERENCES....7
APPENDIX 1.1: MAP OF TERRAIN COVERAGE AND DATA SOURCES....8

CHAPTER 2: TUMMEL FAULT ZONE: A PERMIAN-TRIASSIC STRUCTURE JUXTAPOSING CASSIAR AND YUKON-TANANA TERRANES IN CENTRAL YUKON TERRITORY, CANADA

ABSTRACT....10
INTRODUCTION....11
MAGUNDY REENTRANT AND CASSIAR TERRANE....13
YUKON-TANANA TERRANE....20
Snowcap Complex....21
Drury Formation....21
Pelmac Formation....23
Little Kalzas plutonic suite....23
Little Salmon Formation....25
Summary of Yukon-Tanana evolution recorded in Truitt Creek area....29
TUMMEL FAULT ZONE....29
MID-CRETACEOUS INTRUSIONS....32
STRUCTURE AND METAMORPHISM....34
DISCUSSION....41
SUMMARY....45
REFERENCES....46
APPENDIX 2.1: ANALYTICAL METHODS
Electron microprobe analyses....53
ID-TIMS U-Pb geochronology....53
Geochemical analyses....54

CHAPTER 3: MID-CRETACEOUS PINNING OF ACCRETED TERRANES TO MIOGEOCLINAL ASSEMBLAGES: IRRECONCILEABLE WITH PALEOMAGNETIC DATA?

ABSTRACT....56
INTRODUCTION....57
TECTONIC ELEMENTS IN CENTRAL YUKON....59
SOLITARY MOUNTAIN....60
GEOLOGICAL EVOLUTION RECORDED IN TRUITT CREEK AREA....61
GLENLYON BATHOLITH: A MID-CRETACEOUS PIN....63
DISCUSSION....65
CONCLUSIONS....68
ACKNOWLEDGEMENTS....69
REFERENCES....70

CHAPTER 4: CONCLUSIONS

CONTRIBUTIONS OF THE STUDY....74

Appendix 1:
Geological map of Truitt Creek (NTS 105L/1), central Yukon (1:50 000 scale), Yukon Geological Survey Open File 2002-5 (in pocket)

Appendix 2:
Digital Appendices, CD ROM (in pocket)

LIST OF TABLES

CHAPTER 3

Table 2.1: Geochemical data from volcanic rocks of the Tummel Fault zone and the Lokken Formation and from amphibolite samples from Cassiar terrane....17

Table 2.2: U-Pb analytical data for four samples from Truitt Creek area....26

Table 2.3: Geothermobarometry results from country rock samples adjacent to Glenlyon Batholith....37

Table 2.4: Oxide percent data by mineral from electron microprobe analyses....38

LIST OF FIGURES

CHAPTER 2

Figure 2.1: Simplified terrane map of southern Yukon and regional tectonic assemblage map....12

Figure 2.2: Geological map and cross-section of Truitt Creek area (modified after Gladwin et al., 2002)....14

Figure 2.3: (A) Zr/Ti02 vs Nb/Y diagram showing samples of Tummel fault zone metabasalt, Cassiar terrane amphibolite, and Lokken Member volcanics (diagram after Winchester and Floyd, 1977). (B) V vs Ti/1000 diagram contrasts alkalic amphibolite dykes (triangles) from Cassiar terrane with subalkaline Tummel fault zone metabasalt (diagram after Shervais, 1982). (C) Zr-Nb-Y diagram showing mixed MORB and volcanic arc affinity in basalt samples from the Tummel fault zone (after Meschede, 1986)..... 18

Figure 2.4: Primitive mantle-normalized multielement plots (normalized to primitive mantle values of Sun and McDonough, 1989). (A) Amphibolite samples from Truitt Creek area are superimposed on range of analyses from volcanic rocks of Menzies Creek Formation from the Faro region (shaded area; data from L.C. Pigage, pers. comm., 2002). (B) Volcanic rocks from the Lokken Formation. (C) Basalt samples from the Tummel fault zone. (D) Samples from the Tummel fault zone with a negative Nb anomaly..... 19

Figure 2.5: (A) Light bands of quartzite intercalated with thin bands of chlorite schist from the Pelmac Formation. (B) Basal quartzite pebble to cobble conglomerate from the Little Salmon Formation. (C) Raised dark spots (circled) in serpentinite represent serpentine pseudomorphs after pyroxene. (D) Photomicrograph of holly-leaf texture in serpentinite from the Tummel fault zone. Magnetite (Mg; after spinel) is surrounded by a halo of chlorite (Chl; after plagioclase). (E) A phyllonite outcrop marks a west-dipping thrust fault that indicates a component of ductile deformation in the evolution of the Tummel fault zone. (F) Thick sills of granite separated by thin layers of quartz-mica schist dip moderately to the southwest, suggesting an overall sheetlike geometry of the batholith..... 24

Figure 2.6: U-Pb concordia diagrams: (A) Hornblende granodiorite sample KG01-220 of the Little Kalzas suite. (B) Granodiorite sample 99MC014 taken along Robert Campbell Highway. (C) Basalt sample KG02-048 from the Tummel fault zone. (D) hornblende leucogabbro sample KG01-188 from the Tummel fault zone..... 27

Figure 2.7: Geothermometry and geobarometry diagrams: (A) Sample KG01-155. (B) Sample RB01-004. (C) Sample RB02-012. (D) Samples plotted in P-T space are broadly consistent with lower amphibolite facies metamorphic conditions..... 39

CHAPTER 3

Figure 3.1: A. Geographic distribution of Cassiar (CT), Yukon-Tanana (Y-T), and Slide Mountain (SM) terranes, Selwyn Basin (SB), and Mackenzie Platform (MP), with 425 km of dextral strike-slip motion restored on Tintina fault system (modified after Wheeler and McFeely, 1991). Distribution of 70 Ma Carmacks Group volcanic rocks is shown in black (modified after Wynne et al., 1998). B. Schematic cross-sectional representation of Cassiar platform (CP) and Selwyn Basin with respect to Mackenzie platform.....58

Figure 3.2: Map of Yukon Territory showing regional distribution of mid-Cretaceous intrusions (shaded areas); thick dashed line indicates eastern extent of magmatism (modified after Woodsworth et al., 1991).....58

Figure 3.3: Bedrock geology of Truitt Creek map area. Tectonic element diagram (inset) modified after Gordey and Makepeace (2000)..... 62

ACKNOWLEDGEMENTS

I thank Stephen Johnston, Maurice Colpron, and Robin Black for their contributions to the project. Thanks also to Joe, Dante, Sussi, and Amanda. I appreciate the discussions, favours, information, expertise, suggestions, proofreading, places to stay, pub discussions, eartime, music, and good coffee, from these and many other people.

CHAPTER 1

Introduction

Regional geology

Yukon-Tanana Terrane underlies much of southwestern Yukon Territory, as well as adjacent parts of Alaska and British Columbia. A northwest-trending fault system (the Tummel fault zone) regionally separates Devonian-Mississippian metasedimentary and metaigneous rocks of Yukon-Tanana Terrane to the southwest from lower Paleozoic miogeoclinal metasedimentary rocks of Cassiar Terrane to the northeast (Gordey and Makepeace, 2000). A Permian ophiolitic assemblage correlated with Slide Mountain terrane characterizes the Tummel fault zone. The northwest-trending Tintina fault is an Eocene feature that truncates the northern end of the Tummel fault zone. This study focuses on the Truitt Creek map area (NTS 105L/1, 1:50 000 scale) in southern central Yukon. The Truitt Creek area was initially mapped in the 1950s as part of the Glenlyon geological mapping project (NTS 105L, 1:250 000 scale; Campbell, 1967). Bedrock geological mapping of Truitt Creek map area in 2001 and 2002 has provided constraints on the nature of and amount of displacement across the Tummel fault zone, with implications for (1) the timing of accretion of Yukon-Tanana to continental margin assemblages, and (2) interpretation of Late Cretaceous paleomagnetic data.

Geology of the study area

The lower of the two units exposed in Cassiar terrane in the northwestern part of the map area includes phyllite and pelitic and psammitic schist, with quartzite and marble intercalations. This is conformably overlain by a massive marble unit. These two units record a basin-to-platform facies change during Paleozoic time.

In the southwestern part of the map area, quartzofeldspathic schist of the Snowcap Complex forms the basement to Yukon-Tanana terrane stratigraphy. The Snowcap Complex is overlain by Late Devonian-Mississippian siliciclastic and volcanic rocks of the Drury Formation, which in turn is overlain by quartzite of the Early Mississippian Pelmac Formation. Quartz diorite and tonalite of the ca. 348 Ma Little Kalzas plutonic suite, which is the intrusive root to the Little Kalzas arc exposed to the north (Colpron et al., 2002), intrude these units. The Little Salmon formation is the uppermost unit exposed in Yukon-Tanana stratigraphy, and includes a basal conglomerate and quartz-chlorite schist overlain by marble and intermediate volcaniclastic rocks. Intermediate plutonic rocks of the ca. 338-340 Ma Little Salmon plutonic suite intrude the older rocks. Greenschist facies (biotite grade) regional metamorphism during Jurassic time (Oliver, 1996) produced a well-developed schistosity in Yukon-Tanana rocks that has been folded in broad, open folds.

The Tummel fault zone is a 3 km wide belt defined by an Early Permian unit of basalt, greenstone, and structurally imbricated harzburgite, with an overlying chert-dominated unit that also includes slate and quartzite. An early schistosity has been transposed into parallelism with the dominant schistosity, which is defined by an upper

greenschist facies metamorphic assemblage of epidote + actinolite. Mylonitic and cataclastic textures locally overprint schistosity, recording both ductile and brittle components in the evolution of the Tummel fault zone.

Glenlyon Batholith is a composite intrusion with an early hornblende granodiorite phase that was succeeded by biotite ± muscovite granite, and late pegmatite dykes. K-Ar and Ar-Ar cooling ages from the batholith and adjacent hornfels give a ca. 105 Ma age. U-Pb zircon-dated 105 Ma leucogabbro and hornblende diorite intrusions within the Tummel fault zone are satellites of the main Glenlyon body. Contact metamorphism attributable to Glenlyon magmatism has produced a contact aureole that is characterized by mica ± garnet schist adjacent to the batholith, with andalusite and cordierite porphyroblasts overprinting fabric in country rocks,

Carmacks Group paleomagnetic data

The Carmacks Group consists of unaltered Late Cretaceous volcanic rocks that disconformably overlie much of southwestern Yukon Territory. The easternmost Carmacks Group occurrence is at Solitary Mountain, ~2 km west of the Tummel fault zone. Calculated paleolatitudes from recent paleomagnetic studies of Carmacks Group rocks, including data from Solitary Mountain, require large-scale (1750 ± 550 km) displacement since Late Cretaceous time (Marquis and Globerman, 1988; Wynne et al., 1998). Tintina fault system, the only recognized geological structure east of Solitary Mountain that has accommodated significant lateral motion, records ~425 km of dextral strike-slip displacement (Murphy and Mortensen, 2003; Roddick, 1967). If the

paleomagnetically calculated paleolatitude is correct, northward translation of Yukon-Tanana Terrane requires a major Late Cretaceous – Paleogene structure northeast of Solitary Mountain that has accommodated the remaining ~1325 km displacement.

The Tummel fault system is a structural break northeast of Solitary Mountain, and was thus a candidate to accommodate this "missing" displacement. However, this study has shown that no significant displacement has been accommodated by the Tummel fault zone since ca. 105 Ma, when Glenlyon Batholith and its satellite intrusions were emplaced in Cassiar terrane and the Tummel fault zone, imposing a contact aureole that extends into Yukon-Tanana terrane.

Study overview

Findings of the study are presented in two papers (Chapters 2 and 3). Chapter 2, entitled "Tummel fault zone: A Permian-Triassic structure juxtaposing Cassiar and Yukon-Tanana terranes in central Yukon Territory, Canada," establishes the stratigraphic, metamorphic, and deformational history of each tectonic element present in the Truitt Creek area, and uses these histories to constrain amalgamation of these elements to Permian-Triassic time. Chapter 3, "Mid-Cretaceous pinning of accreted terranes to miogeoclinal assemblages in the northern Cordillera: Irreconcilable with paleomagnetic data?", examines the tectonic implications of this study with respect to Late Cretaceous paleomagnetic data from volcanic rocks that overlie Yukon-Tanana terrane. Because amalgamation of Yukon-Tanana and Cassiar terranes pre-dates the Carmacks Group paleomagnetic data, large-scale translations required by these data must be applied to Cassiar terrane as well. Interpretation of Cassiar terrane as being far-travelled is contrary

to interpretations of it as parautochthonous (North American) miogeocline (Gordey and Anderson, 1993).

Methodology

Fieldwork was completed during six weeks in July and August 2001 and four weeks in July 2002. Traverses were carried out by myself and an assistant (Robin Black) on foot from a base camp that was placed and moved each five to seven days by helicopter. Base camp locations were chosen to provide opportunities to locate and follow lithological contacts while maximizing coverage of the area (according to availability of outcrop; Appendix 1.1). Additional traverses were conducted from the shores of Little Salmon Lake, accessed by motorboat, and from Robert Campbell Highway, accessed by truck. Lithological and structural data, as well as samples for later laboratory analyses, were collected on traverse.

The papers in chapters 2 and 3 are based upon a geological map of the study area (Appendix 1, in pocket) that I compiled from interpretations of my observations and data supplemented with other workers' observations (see contribution map, inset, in Appendix 1, in pocket). Subsurface interpretations (shown in cross-section diagrams in Figure 2.2 and Appendix 1, in pocket) are inferred from my structural data and field relationships. The map was prepared from a digital topographic base map (from the Surveys and Mapping Branch, Department of Mines, Energy, and Resources), using Autodesk Map 5.0 software. A database including all data and observations from fieldwork and thin sections was prepared using GeoField software (a Microsoft Access-based template from Yukon Geological Survey).

Samples for thin section were chosen, slabbed, and analyzed by myself. Samples of metabasalt from the Tummel fault zone and amphibolite from the Kechika Group were chosen and prepared for geochemical analysis by myself. Geochemical data from the Lokken Member were contributed by Maurice Colpron (Yukon Geological Survey). Geochemical plots in Chapter 2 were prepared using Microsoft Excel software.

Geothermobarometric data and interpretations in Chapter 2 were contributed by Robin Black (his B.Sc. Honours thesis; Black, 2002); methodology is outlined in Appendix 2.1. Geochronological data and interpretations presented in Chapter 2 were contributed by J.K. Mortensen (University of British Columbia); methodology is given in Appendix 2.1.

References

Black, R., 2002, Geology and metamorphism of Cassiar terrane, Truitt Creek map sheet (105L/1), south-central Yukon [B.Sc. Honours thesis]: University of Victoria, 32 p.

Campbell, R. G., 1967, Geology of Glenlyon map-area, Yukon Territory (105L), Geological Survey of Canada, 92 p.

Colpron, M., Murphy, D. C., Nelson, J. L., Roots, C. F., Gladwin, K., Gordey, S. P., Abbott, G., and Lipovsky, P. S., 2002, Preliminary geological map of Glenlyon (105L/1-7, 11-14) and northeast Carmacks (115I/9, 16) areas, Yukon Territory: Geological Survey of Canada, scale 1:125 000.

Gordey, S. P., and Anderson, R. G., 1993, Evolution of the northern Cordilleran miogeocline, Nahanni map area (105I), Yukon and Northwest Territories: 214, Geological Survey of Canada, 214 p.

Gordey, S. P., and Makepeace, A. J., 2000, Bedrock Geology, Yukon Territory: Exploration and Geological Services Division, Yukon Region, Indian and Northern Affairs Canada, scale 1:1 000 000.

Marquis, G., and Globerman, B. R., 1988, Northward motion of the Whitehorse Trough: paleomagnetic evidence from the Upper Cretaceous Carmacks Group: Canadian Journal of Earth Sciences, v. 25, p. 2005-2016.

Oliver, D. H., 1996, Structural, kinematic, and thermochronologic studies of the Teslin suture zone, south-central Yukon Territory [Ph.D. thesis]: Southern Methodist University, 231 p.

Wynne, P. J., Enkin, R. J., Baker, J., Johnston, S. T., and Hart, C. J. R., 1998, The Big Flush - Paleomagnetic signature of a 70 Ma regional hydrothermal event in displaced rocks of the northern Canadian Cordillera: Canadian Journal of Earth Sciences, v. 35, p. 657-671.

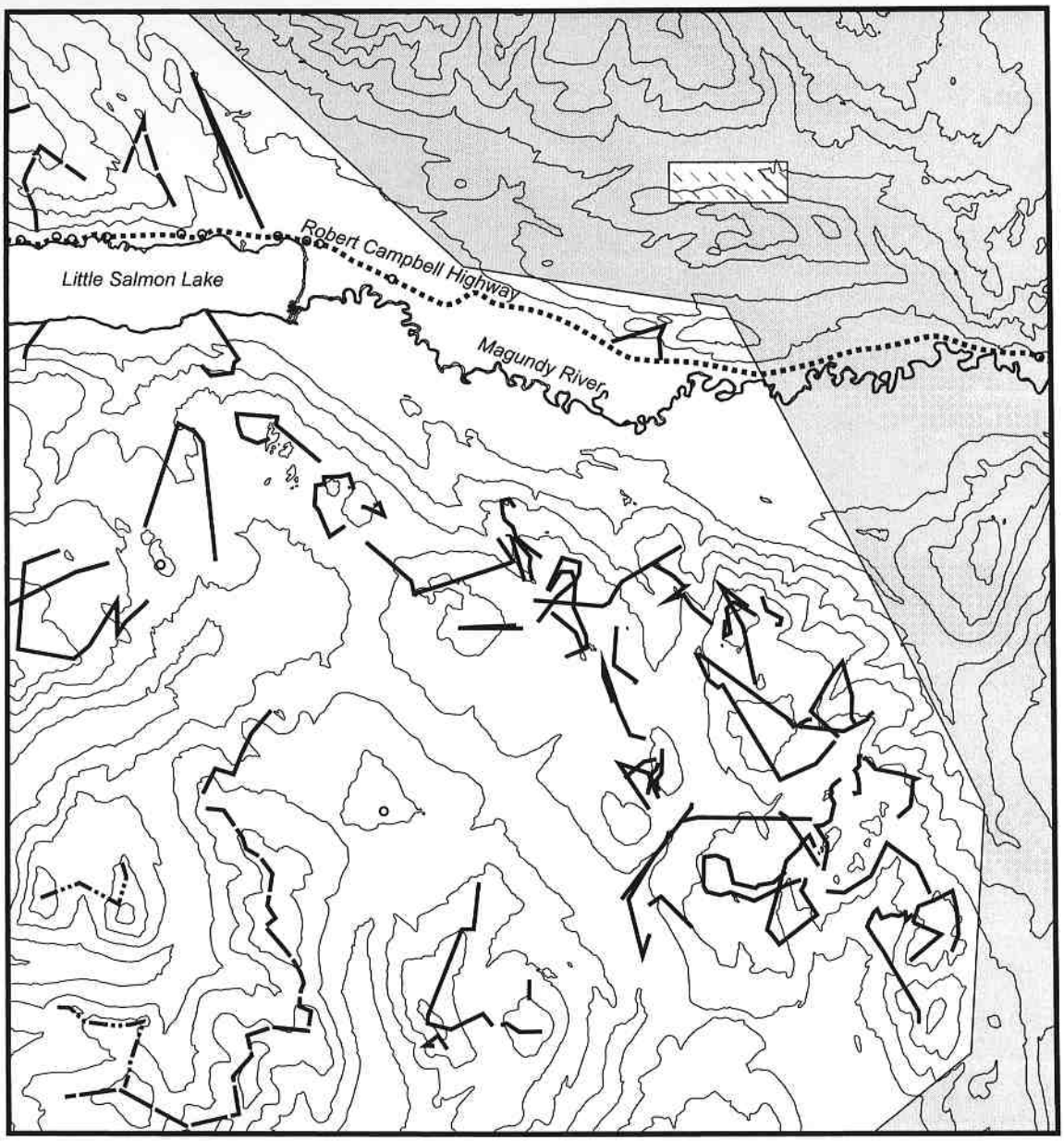

Helicopter or truck stop
This study
Traverses by M.Colpron, 1999-2002
Traverses by D. Murphy, C. Roots, 2002
Data from Campbell (1967)
Data from Paterson (1982 Assessment Report 091372)

Appendix 1.1: Terrain coverage and data sources for geological map of Truitt Creek area.

CHAPTER 2

Tummel fault zone: a Permian-Triassic structure juxtaposing Cassiar and Yukon-Tanana terranes in central Yukon Territory, Canada

Gladwin, K., School of Earth and Ocean Sciences, University of Victoria, P.O. Box 3055 STN CSC, Victoria, British Columbia V8W 3P6, kaesy@uvic.ca

Colpron, M., Yukon Geological Survey, P.O. Box 2703 (K-10), Whitehorse, Yukon, Canada Y1A 2C6, maurice.colpron@gov.yk.ca

Johnston, S.T., School of Earth and Ocean Sciences, University of Victoria, P.O. Box 3055 STN CSC, Victoria, British Columbia V8W 3P6, stj@uvic.ca

Mortensen, J.K., Department of Earth and Ocean Sciences, University of British Columbia, Vancouver, British Columbia, Canada V6T 1Z4, jmortensen@eos.ubc.ca

and

Black, R., Department of Geology, Acadia University, Wolfville, Nova Scotia, Canada B0P 1X0, 062870b@acadiau.ca

December 2003 7095 words

Corresponding author:

Kaesy Gladwin Phone: (250) 472-4011; Fax: (250) 721-6200
kaesy@uvic.ca

Abstract

This paper reports on geological mapping across the Tummel fault zone (TFZ), which defines a section of the boundary between continental margin assemblages assigned to Cassiar terrane and clastic and magmatic arc rocks of Yukon-Tanana terrane in southern central Yukon Territory. The TFZ is defined by a northwest-trending belt of ca. 267 Ma greenstone, chert, and harzburgite that is correlated with assemblages of Slide Mountain terrane. Northeast of the TFZ, a Paleozoic continental platform assemblage (Cassiar terrane) includes phyllite, pelitic and psammitic schist (Kechika Group), and an upper homogeneous marble unit (Askin Group). Southwest of the TFZ, Yukon-Tanana terrane consists of quartzofeldspathic basement (the Snowcap Complex) overlain by Upper Devonian to Mississippian siliciclastic and volcanic rocks (the Drury Formation and Lokken Member, respectively) and by the Lower Mississippian Pelmac Quartzite. These units are intruded by granodiorite and tonalite of the ca. 343-349 Ma Little Kalzas arc plutonic suite. Immature clastic, carbonate, and intermediate volcaniclastic rocks of the Little Salmon Formation overlie the older units, and are intruded by intermediate plutonic rocks of the ca. 339 Ma Little Salmon plutonic suite.

The Glenlyon Batholith and its 105 Ma satellite plutons intrude Cassiar terrane and the TFZ. Muscovite + biotite + andalusite ± garnet ± cordierite mineral assemblages and margin-parallel schistosity define a contact metamorphic aureole that extends from Cassiar terrane across the TFZ and into Yukon-Tanana terrane, indicating that intrusion postdates terrane amalgamation.

Introduction

How continents grow remains a fundamental problem in the earth sciences. The Cordilleran orogen of western North America is interpreted as an example of continental growth by terrane accretion along a long-lived convergent margin (e.g. Coney et al., 1980). One way to test and constrain this model is to examine the structures that juxtapose accreted terranes with each other and with North American stratigraphy. Toward this goal, we conducted a geological mapping program in the Truitt Creek map area (NTS 105L/1) in central Yukon Territory examining the eastern boundary of the most inboard of the accreted terranes.

In the study area, rocks of Yukon-Tanana terrane are juxtaposed with Cassiar terrane (Fig. 2.1). Cassiar terrane consists of a lower Paleozoic continental margin succession that is generally interpreted as a parautochthonous segment of the North American miogeocline (e.g. Fritz et al., 1991; Wheeler and McFeely, 1991), but has also been interpreted as a far-travelled section of North American margin (Pope and Sears, 1997) or as a segment of miogeocline that is exotic with respect to North America (Johnston, 2001). Mid-Paleozoic metasedimentary and metaigneous rocks constitute Yukon-Tanana terrane, interpreted as the easternmost of the terranes added to the Paleozoic western margin of North America (e.g. Coney et al., 1980; Wheeler and McFeely, 1991). A 2-3 km wide northwest-trending belt of basalt and chert characterizes the Tummel fault zone, which separates Yukon-Tanana terrane to the southwest from Cassiar terrane to the northeast. The northern end of the Tummel fault zone is truncated by the Big Salmon fault (Fig. 2.1; Colpron et al., 2002).

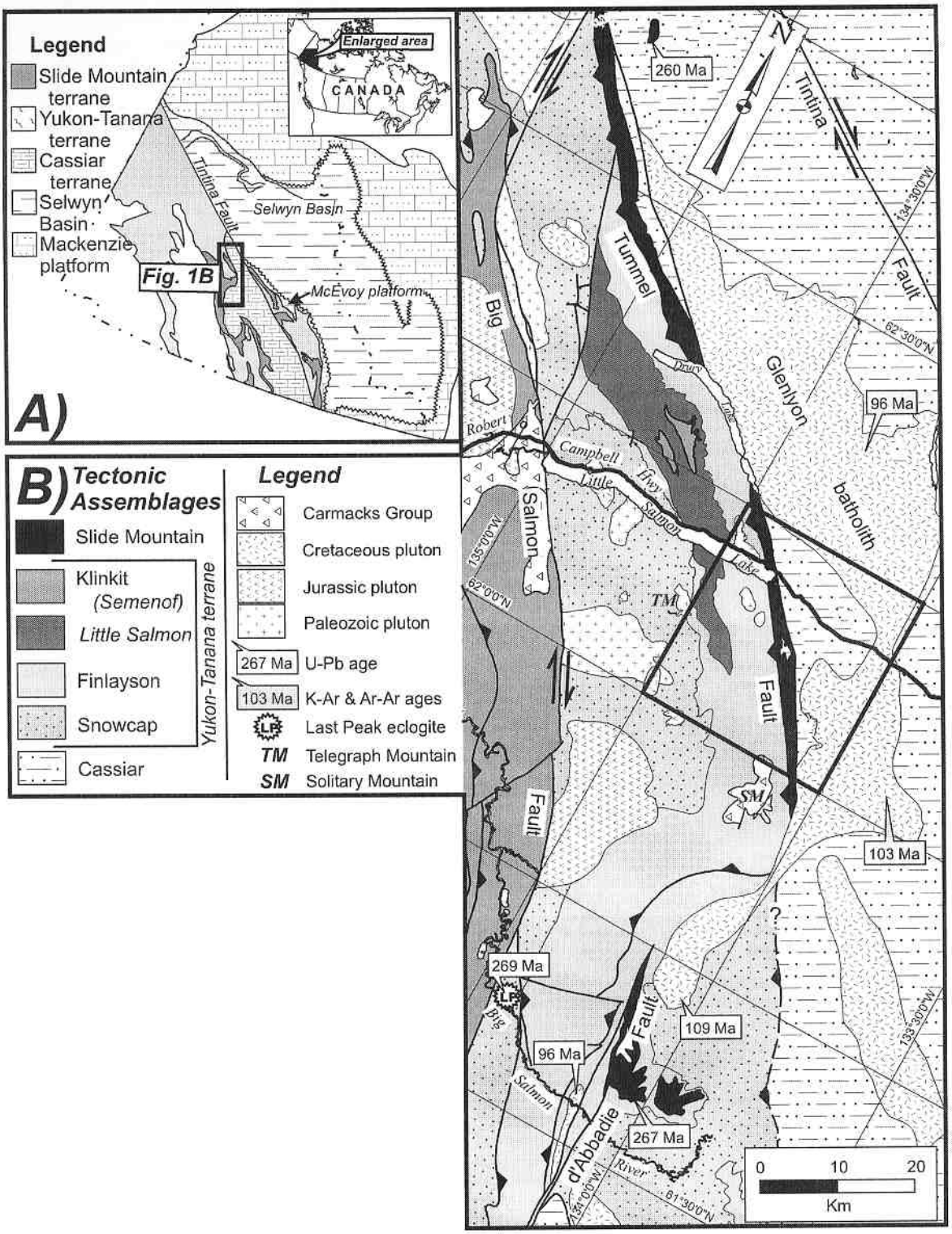

Figure 2.1: (A) Simplified terrane map of southern Yukon, modified after Wheeler and McFeely (1991). (B) Regional tectonic assemblage map after Colpron et al. (in review-b). Study area outlined in black.

We report here the results of our geological mapping, providing detailed geological descriptions of the Cassiar and Yukon-Tanana terranes and of the Tummel fault zone. We use these data to: (1) characterize each of the tectonic elements present in the study area; (2) constrain the geotectonic evolutions that these elements record; and (3) discuss the nature and significance of the Tummel fault zone which juxtaposes these elements. In addition to better constraining the tectonic evolution of the northern Cordillera, our results have implications for understanding the processes involved in continental growth.

Magundy reentrant and Cassiar terrane

Dark pelitic rocks and grey marble exposed along Magundy River and bound by the Glenlyon batholith to the east and the Tummel fault zone to the west are referred to as the Magundy reentrant (Fig. 2.2). Campbell (1967) inferred that these rocks (his units 8a and 8b) were separated from schist and granitic rocks to the east by faults, but acknowledged that they might be less-metamorphosed equivalents of those schistose rocks (his units 2-4; Harvey Group). Gordey and Makepeace (2000) assigned rocks of the Magundy reentrant to the Anvil assemblage (their unit CPA) of Slide Mountain terrane, because the dominantly pelitic protolith suggests a basinal setting. These rocks are here considered part of Cassiar terrane for reasons discussed below.

Along Robert Campbell highway (Fig. 2.2), the pelitic rocks consist of grey to black, locally calcareous, commonly iron oxide-stained phyllite. To the southeast, the pelitic rocks are metamorphosed to quartz + muscovite ± biotite ± garnet schist in the contact aureole of the Glenlyon Batholith, intercalated with subordinate pale green to white quartzite, marble, calc-silicate rocks, and amphibolite. Amphibolite occurs as 1-5 m thick

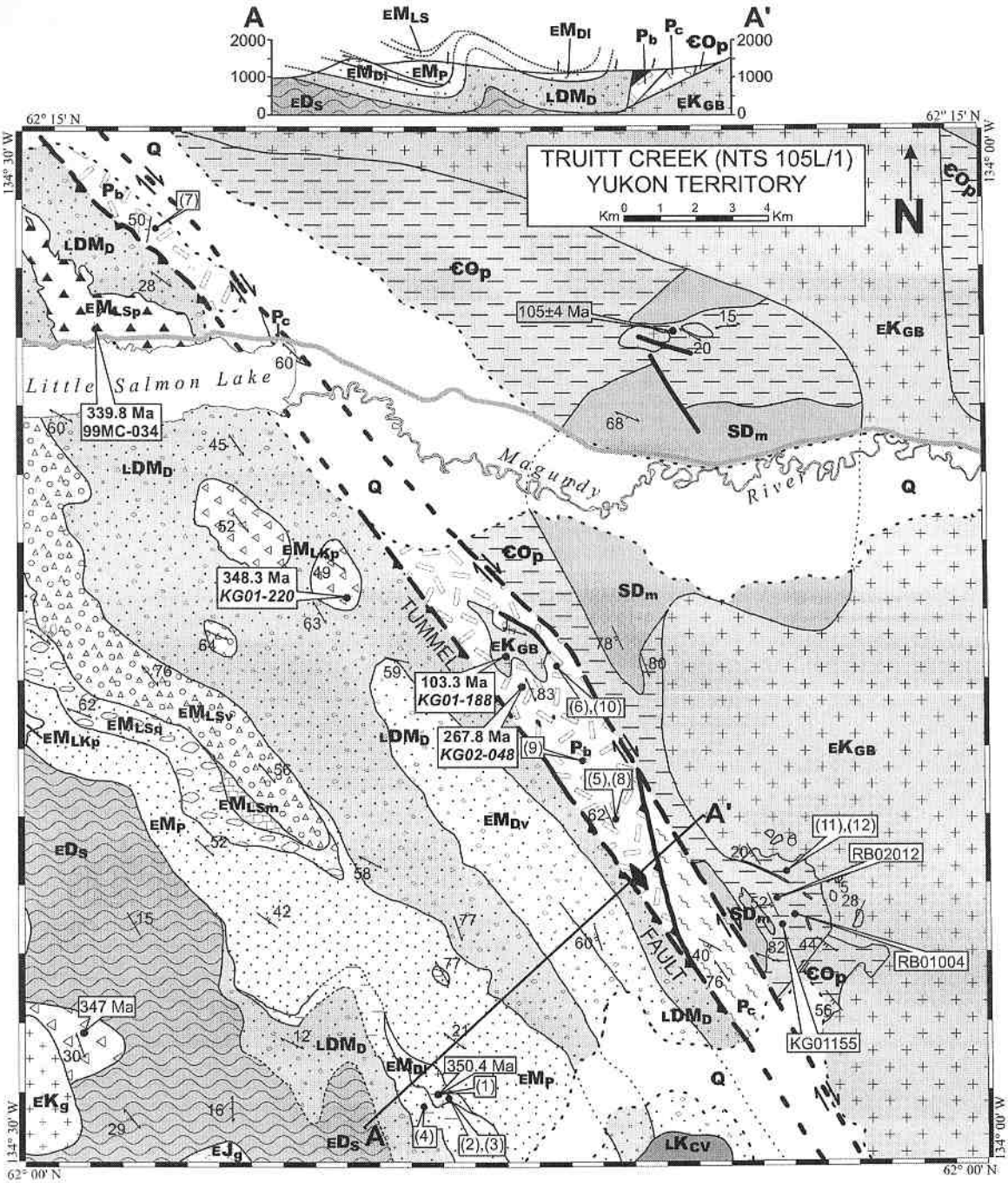

Figure 2.2: Geological map and cross-section of Truitt Creek area. (Location shown in Fig. 2.1; modified after Gladwin et al., 2002).

LEGEND

Q — **Quaternary**
Unconsolidated alluvium, colluvium, glacial deposits

OVERLAP ASSEMBLAGE

INTRUSIVE ROCKS

$_{E}K_{GB}$ — **Early Cretaceous**
Biotite granite, biotite-muscovite granite, plagioclase-muscovite pegmatite, hornblende leucogabbro

$_{E}K_{g}$ — **Early Cretaceous**
Biotite granite

$_{E}J_{g}$ — **Early Jurassic (?)**
Hornblende-biotite gabbro

LAYERED ROCKS

$_{L}K_{CV}$ — **Late Cretaceous**
Carmacks Group - basalt flows, agglomerate

TUMMEL FAULT ZONE

P_{c} — **Lower Permian**
White, green, & black chert, quartzite, black slate

P_{b} — **Lower Permian**
Basalt, greenstone; coarse-grained serpentinized harzburgite (*in black*)

Dextral strike-slip fault

Geological contact

Inferred thrust fault

105±4 Ma — K-Ar cooling age

348.3 Ma — U-Pb zircon age date *(bold text indicates samples discussed in text)*

(3) — Geochemistry sample

RB02012 — Geothermobarometry sample

62 — Bedding

40 — Compositional layering

45 — Foliation

YUKON-TANANA TERRANE

INTRUSIVE ROCKS

Little Salmon plutonic suite

$_{E}M_{LSp}$ — **Early Mississippian**
hornblende quartz diorite, granodiorite

Little Kalzas plutonic suite

$_{E}M_{LKp}$ — **Early Mississippian**
hornblende-biotite granodiorite, quartz diorite and tonalite

LAYERED ROCKS

Little Salmon Formation

$_{E}M_{LSv}$ — **Lower Mississippian**
Mint-green banded metavolcaniclastic rocks

$_{E}M_{LSq}$ — **Lower Mississippian**
Quartzite-clast conglomerate, quartz-chlorite schist; marble

Pelmac Formation

$_{E}M_{P}$ — **Lower Mississippian**
Quartzite, quartz-mica schist

Drury Formation

$_{E}M_{DIp}$, $_{E}M_{DI}$ — **Lower Mississippian**
Lokken member - (lower) Intermediate volcaniclastic rocks, minor marble and psammite; *(upper)* quartz-feldspar porphyry, volcaniclastic rocks

$_{L}DM_{D}$ — **Upper Devonian - Mississippian**
Arkosic grit, quartzite, psammite, marble

Snowcap Complex

$_{E}D_{S}$ — **Pre-Upper Devonian**
Quartzite, psammitic and pelitic schist

CASSIAR TERRANE

Askin Group

SD_{m} — **Silurian - Devonian**
Marble, calc-silicate rocks, quartz-mica schist

Kechika Group

ϵO_{p} — **Cambrian - Ordovician**
Phyllite, quartz-mica schist, quartzite, marble, amphibolite

parallel layers and crosscutting bodies with respect to compositional layering in pelitic and calc-silicate schist of the southeastern part of the study area. The amphibolite was deformed and metamorphosed along with the host rock, and are interpreted as mafic dykes that intruded the pelitic rocks. Two samples of amphibolite were analysed for major and trace element geochemistry (Table 2.1; samples 11, 12). They have compositions typical of alkali basalt of within-plate affinity (Fig. 2.3). On primitive mantle-normalized plots, the amphibolite samples display enrichments in incompatible elements typical of ocean-island basalt (Fig. 2.4A).

Their trace element signature resembles that of volcanic rocks of the Cambrian-Silurian Menzie Creek Formation in the Faro district, northeast of the Tintina fault (Fig. 2.1, 2.4A). The Menzie Creek Formation is part of a suite of alkalic magmatic rocks that occur sporadically in continental margin strata of the northern Cordillera, interpreted as rift volcanic rocks that were emplaced during intermittent Lower Paleozoic extension within the miogeocline (Goodfellow et al., 1995). The amphibolite dykes in the Truitt Creek area may be feeders to Menzie Creek-equivalent rift volcanic rocks.

The pelitic rocks are gradationally overlain by fine- to coarse-grained, light grey to black, locally graphitic marble of the Askin Group (Fig. 2.2). The contact relationship between the two units is best exposed in the southeastern part of the map area, where 5-50 cm thick layers of siliceous and calcareous metasedimentary rocks are intercalated over 50-70 metres. Near the highway, the marble is massive, fine-grained, dark grey to black, and heavily veined with calcite. In the central and southeastern parts of the map area, the marble is homogeneous, massive, medium- to coarse-grained and grey to white in colour.

SAMPLE	02DM 001-3	01MC 287	01MC 288	01MC 288B	01MC 287B	KG01 024	KG01 031	99MC 188	KG01 025F	KG01 029	KG01 185	02JN 003	KG01 154	KG01 153
Label[1]	-	*(1)*	*(2)*	*(3)*	*(4)*	*(5)*	*(6)*	*(7)*	*(8)*	*(9)*	*(10)*	-	*(11)*	*(12)*
Unit[2]	Lp	Lp	Lp	Lp	Lb	TFZb	TFZb	TFZb	TFZb	TFZb	TFZb	TFZb	CTa	CTa
SiO2	69.26	78.06	70.32	69.73	47.79	61.64	56.69	61.16	48.37	49.55	48.86	51.79	48.87	48.60
Al2O3	14.32	9.00	14.85	15.27	16.35	15.10	16.42	15.69	17.57	17.32	16.33	14.09	12.30	13.90
Fe2O3	3.58	2.11	2.74	2.61	9.99	7.63	8.89	7.05	9.13	7.29	9.88	10.93	14.04	15.11
MnO	0.060	0.056	0.059	0.053	0.155	0.150	0.217	0.06	0.122	0.140	0.171	0.17	0.29	0.22
MgO	1.71	0.75	0.79	0.85	8.38	2.53	3.70	3.00	7.38	8.18	8.49	7.84	4.10	4.35
CaO	2.18	2.68	2.03	1.71	12.22	5.75	3.85	1.81	8.02	10.76	6.82	6.48	9.57	8.27
Na2O	4.88	1.27	3.25	3.15	2.03	2.62	3.59	4.79	2.87	2.62	4.08	4.6	2.58	2.72
K2O	1.39	2.47	3.06	3.52	0.23	1.10	1.50	3.28	0.95	1.06	0.29	0.28	1.38	1.11
TiO2	0.45	0.27	0.30	0.30	0.94	0.961	0.974	1.14	0.633	0.489	1.484	1.42	2.63	3.09
P2O5	0.10	0.06	0.07	0.09	0.11	0.25	0.19	0.42	0.04	0.05	0.32	0.15	1.22	0.71
LOI	1.53	2.25	1.50	1.68	0.79	2.36	3.62	2.10	4.85	2.85	3.49	2.46	1.99	0.95
TOTAL	*99.45*	*98.99*	*98.98*	*98.95*	*98.98*	*100.09*	*99.65*	*100.48*	*99.94*	*100.31*	*100.22*	*100.19*	*98.98*	*99.03*
V	47.61	32	36	41	277	144	202	77	208	148	196	280	196	343
Cr	n.d.	19	19	13	380	29.9	33.3	n.d.	73.8	371.8	266.0	194.3	32	32
Co	6.55	n.d.	5	n.d.	42	15.7	23.1	11.2	26.9	36.1	38.7	38.4	27	33
Ni	n.d.	23	28	12	175	24.9	20.8	n.d.	26.1	130.9	104.2	84.2	215	58
Cu	n.d.	n.d.	20	n.d	57	113.4	113.4	n.d.	101.3	16.3	26.3	80.5	23	45
Zn	35.67	24	148	101	77	77.5	114.4	67.0	79.7	60.4	100.6	93.7	166	137
Ga	12.87	9.9	15.6	13.3	17	17.9	19.0	16.1	16.7	13.9	15.2	15.2	19.1	24.9
Rb	37.91	78.3	77.6	80.1	5	23.4	36.8	64.4	14.9	24.3	5.4	5.1	56.18	52.88
Sr	78.39	206.3	166.3	161.6	180	141	367	235	96	191	145	150	133.5	308.3
Y	18.11	21.6	19.1	20.4	25.7	30.2	24.6	29.4	10.2	10.3	32.1	31.5	58.3	50.3
Zr	160.89	209	104	107.8	55	167.3	113.6	382.3	51.5	26.2	179.3	99.0	305.7	281.2
Nb	9.10	8.13	11.04	11.85	13.4	8.1	4.3	22.4	1.6	1.4	22.9	2.7	39.9	35
Cs	0.30	1.51	1.19	1.67	0.3	1.1	0.9	2.0	1.0	0.9	0.1	0.7	1.65	>5.00
Ba	463	897	880	1061	106	644	1400	2230	991	302	208	414	338	359
Hf	3.96	5.1	3.27	3.28	1.7	4.2	2.8	9.2	1.4	0.7	3.8	2.5	6.86	4.44
Ta	0.81	0.71	0.93	1.02	0.73	0.5	0.3	1.6	0.0	0.1	1.6	0.1	2.35	2.15
Th	9.19	15.06	13.34	13.34	1.05	3.7	1.9	18.0	0.3	0.2	2.4	0.3	6.95	5.09
U	2.50	2.26	2.25	2.21	0.31	1.3	0.8	4.5	0.1	0.1	0.8	0.2	1.68	1.33
La	23.10	30.06	29.16	24.21	7.8	19.18	12.44	66.34	1.19	1.50	18.91	5.07	45.65	37.04
Ce	42.75	62.03	51.75	39.58	15.7	42.06	28.26	119.98	3.29	3.89	38.53	13.79	98.27	80.06
Pr	4.41	6.49	5.58	4.22	2.04	5.21	3.39	13.38	0.52	0.55	4.41	2.02	13.39	10.88
Nd	16.41	22.74	18.05	13.84	9.2	23.24	15.39	48.14	2.73	2.98	20.12	10.86	57.82	45.64
Sm	3.26	3.63	3.28	2.6	2.51	5.28	3.79	8.39	0.95	1.00	5.27	3.42	12.86	10.48
Eu	0.86	0.77	0.97	0.77	1.06	1.52	1.22	2.37	0.64	0.57	1.88	1.26	4.17	3.5
Gd	3.17	2.87	2.67	2.21	3.42	5.19	3.93	6.93	1.24	1.34	5.63	4.25	13.19	10.78
Tb	0.51	0.38	0.43	0.36	0.62	0.87	0.68	1.04	0.27	0.27	0.97	0.83	1.92	1.64
Dy	3.13	2.24	2.44	2.08	4.01	5.35	4.28	5.60	1.77	1.80	5.97	5.44	10.86	9.46
Ho	0.61	0.44	0.51	0.45	0.92	1.04	0.84	1.05	0.35	0.36	1.14	1.11	2.14	1.91
Er	2.01	1.29	1.38	1.37	2.58	3.26	2.53	3.05	1.13	1.11	3.33	3.36	5.76	5.14
Tm	0.32	0.2	0.23	0.21	0.390	0.50	0.40	0.47	0.18	0.18	0.49	0.51	0.82	0.73
Yb	2.01	1.36	1.58	1.47	2.50	3.11	2.48	3.14	1.20	1.07	2.96	3.14	4.73	4.31
Lu	0.31	0.221	0.248	0.229	0.383	0.46	0.36	0.48	0.18	0.15	0.42	0.46	0.717	0.649
NTSMap	*105L/7*	105L/1	105L/1	105L/1	105L/1	105L/1	105L/1	105L/1	105L/1	105L/1	105L/1	*105L/7*	105L/1	105L/1
Easting[3]	506732	536872	536988	536988	536552	542673	541219	529448	542673	541214	540910	500914	546587	546587
Northing	6915179	6876423	6876679	6876679	6876589	6883300	6886075	6899214	6883300	6885175	6887525	6921649	6881712	6881532

Notes: [1]Labels show sample locations in Figure 2.2 ("-" indicates a sample from another map sheet). [2]Unit and rock codes: L = Lokken member, TFZ = Tummel fault zone rocks, G = Glenlyon suite, CT = Cassiar terrane. p = porphyry, b = basalt, a = amphibolite. [3]UTM zone 8, NAD83. n.d. = not detectable.

Table 2.1: Geochemical data from volcanic rocks of the TFZ and the Lokken Member and from amphibolite samples from Cassiar terrane.

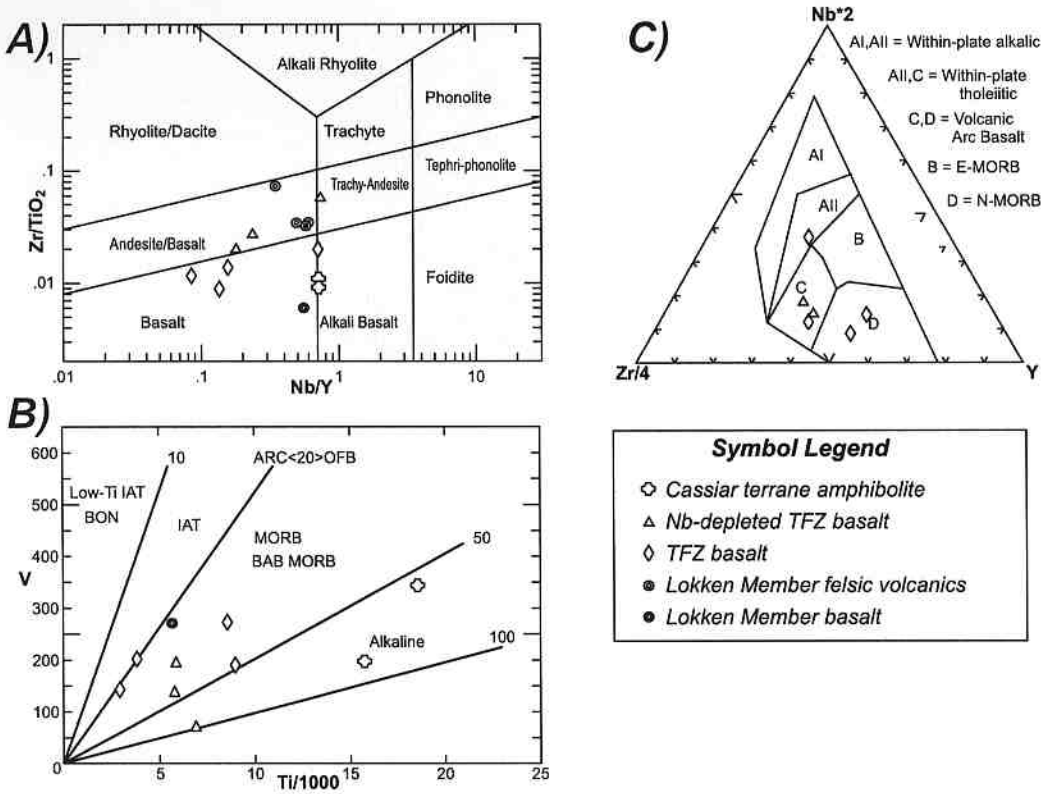

Figure 2.3: (A) Zr/Ti02 vs Nb/Y diagram showing samples of Tummel fault zone metabasalt, Cassiar terrane amphibolite, and Lokken Member volcanics (diagram after Winchester and Floyd, 1977, modified by Pearce, 1996). (B) V vs Ti/1000 diagram contrasts alkalic amphibolite dykes (triangles) from Cassiar terrane with subalkaline Tummel fault zone metabasalt (diagram after Shervais, 1982). (C) Zr-Nb-Y diagram showing mixed MORB and volcanic arc affinity in basalt samples from the Tummel fault zone (after Meschede, 1986).

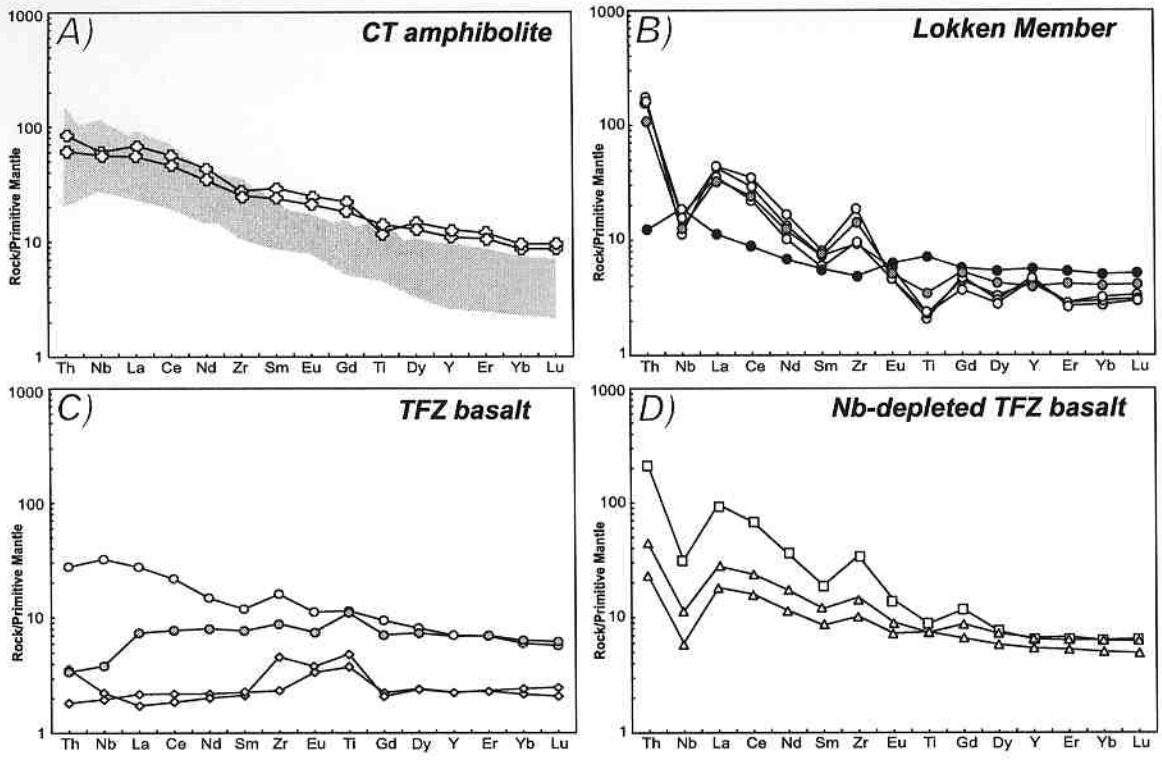

Figure 2.4: Primitive mantle-normalized multielement plots (normalized to primitive mantle values of Sun and McDonough, 1989). (A) Amphibolite samples from Truitt Creek area (Table 2.1, samples 11, 12) superimposed on range of analyses from volcanic rocks of Menzies Creek Formation from the Faro region (shaded area; data from L.C. Pigage, pers. comm., 2002). (B) Volcanic rocks from the Lokken Formation (Table 2.1, samples 1-4 and 02DM001-3). (C) Basalt samples from the Tummel fault zone (Table 2.1, samples 5-7). (D) Samples from the Tummel fault zone with a negative Nb anomaly (Table 2.1, samples 8-10 and 02JN003).

Precise correlation of the pelitic and carbonate rocks of the Magundy reentrant is hampered by a lack of age constraints. A single poorly preserved conodont recovered from a sample of medium-grained marble suggests a Paleozoic age (M.J. Orchard, Geological Survey of Canada Report MJO-2003-08). The dominantly fine-grained pelitic and calcareous protoliths of the Magundy reentrant bear no resemblance to metachert, metavolcanic, and psammitic rocks that comprise the Tummel fault zone and Yukon-Tanana terrane to the west. Rocks of the Magundy reentrant also differ from chert, basalt, and serpentinite characteristic of Slide Mountain terrane (e.g. Division I of Nelson, 1993), and are thus unlikely to be correlative with Slide Mountain terrane as suggested by Gordey and Makepeace (2000). We propose that the calcareous pelite and marble are equivalents of the Kechika and Askin groups, respectively, which are predominant units of Cassiar terrane to the north and east of Glenlyon Batholith (Colpron et al., 2002; Gordey and Makepeace, 2000).

Yukon-Tanana terrane

In Truitt Creek map area, four principal stratigraphic divisions are recognized southwest of the Tummel fault zone in Yukon-Tanana terrane: (1) pre-Upper Devonian metasedimentary and metaplutonic rocks of the Snowcap Complex; (2) Upper Devonian-Lower Mississippian metasedimentary and subordinate metavolcanic rocks of the Drury Formation; (3) Lower Mississippian quartzite of the Pelmac Formation; and (4) middle Mississippian and younger metasedimentary and metavolcanic rocks of the Little Salmon Formation and their subvolcanic intrusions (Fig. 2.2; Colpron et al., in review-a). The

Snowcap Complex and the Drury and Pelmac formations are intruded by intermediate rocks of the Early Mississippian Little Kalzas plutonic suite.

Snowcap Complex

The Snowcap metamorphic complex is the oldest and most extensive unit of Yukon-Tanana terrane in central Yukon (Colpron et al., in review-a; Colpron et al., 2002). In Truitt Creek map area, the Snowcap Complex consists of light grey quartz-muscovite-garnet schist, dark grey quartzite, and minor dark grey carbonaceous schist. These rocks are strongly foliated and coarsely recrystallized, with amphibolite-grade metamorphic mineral assemblages. The Snowcap Complex has experienced a more complex deformational and metamorphic history than overlying Upper Devonian — Mississippian strata. It is intruded by grey hornblende tonalite of the Early Mississippian Little Kalzas plutonic suite and by Early Jurassic gabbro and Early Cretaceous granite (Fig. 2.2). The age of the Snowcap Complex is constrained as pre-Late Devonian by overlying Upper Devonian – Lower Mississippian metasedimentary rocks of the Drury Formation (Colpron et al., in review-a).

Drury Formation

The Drury Formation overlies the Snowcap Complex and includes coarse-grained arkosic grit, light to dark grey quartzite, micaceous quartzite and psammitic schist. In the central part of the study area, a subunit of dark grey to black phyllite and light calcareous metasandstone intercalated with 5- to 20-cm thick layers of light grey marble is recognized (Fig. 2.2).

The top of the Drury Formation consists of mint- to yellow-green intermediate volcanic and volcaniclastic rocks, thinly layered, green to maroon, tuffaceous volcaniclastic rocks, with an upper white, fine- to medium-grained, foliated quartz-feldspar porphyry (the Lokken Member; Fig. 2.2). In some exposures, up to 50% of the porphyry consists of feldspar and quartz phenocrysts. At one locality, 3-5 cm-thick layers of felsic schist are transposed parallel to layering in the surrounding volcaniclastic rocks, representing either depositional intercalations or feeder dykes to the overlying porphyry North of Drury Lake, similar felsic rocks are intercalated with chloritic phyllite and psammitic schist (Colpron et al., in review-a). The porphyry is interpreted as a volcanic horizon because its shallowly-dipping attitude parallels surrounding layers and no cross-cutting relationships were observed. The porphyry unit is 200 m thick and is underlain by 400 m of volcaniclastic rocks, giving the Lokken Member a total thickness of ca. 600 m (Fig. 2.2).

Four samples of felsic volcanic rock and one sample of chlorite schist taken from the Lokken Member were analyzed for major and trace element geochemistry (Table 2.1; samples 1-4 and 02DM001-3). The chlorite schist samples have basaltic compositions on the modified Zr/TiO_2–Nb/Y diagram (Fig. 2.3A) and plot in the E-MORB field on the Zr-Nb-Y diagram of Meschede (1986, Fig. 2.3C). A negative Nb anomaly in primitive mantle-normalized multielement plot profiles of the felsic samples (Fig. 2.3B) indicates that the Lokken Member records arc magmatism.

Quartz-feldspar porphyry samples from the Lokken Member (Fig. 2.2) and from the top of the Drury Formation north of Drury Lake (Fig. 2.1) have yielded concordant U-Pb zircon ages of 350.4 ± 1.3 Ma and 350.5 ± 1.8 Ma, respectively (Colpron et al., in

review-a). Two samples of grit from the Drury Formation have yielded exclusively Late Devonian detrital zircon populations (Colpron et al., in review), consistent with a lower Mississippian depositional age.

Pelmac Formation

The Pelmac Formation unconformably overlies the Snowcap Complex and Drury Formation (Fig. 2.2). It is a distinct and laterally extensive orthoquartzite unit that can be traced into the northwestern part of Glenlyon map area (Colpron et al., 2002). The quartzite is white or pale green and is homogeneous and massive, although locally 2-cm-thick horizons of quartz-chlorite schist are intercalated with 3- to 10-cm-thick quartzite beds (Fig. 2.5A). The age of the Pelmac Formation is tightly constrained as being younger than the underlying 350 Ma Lokken Member, and older than a 348 Ma pluton that intrudes it (described below).

Little Kalzas plutonic suite

Rocks of the Snowcap Complex, Drury Formation, and Pelmac Formation are intruded by the Little Kalzas plutonic suite in the central and western parts of Truitt Creek map area (Fig. 2.2). The suite includes medium to coarse-grained hornblende ± biotite granodiorite and hornblende quartz diorite. A moderate to strong foliation defined by the alignment of chlorite, biotite, and epidote parallels regional foliation in country rock.

A pluton of hornblende granodiorite 5 km south of the eastern end of Little Salmon Lake was sampled for U-Pb geochronology (KG01-220). The sample yielded abundant

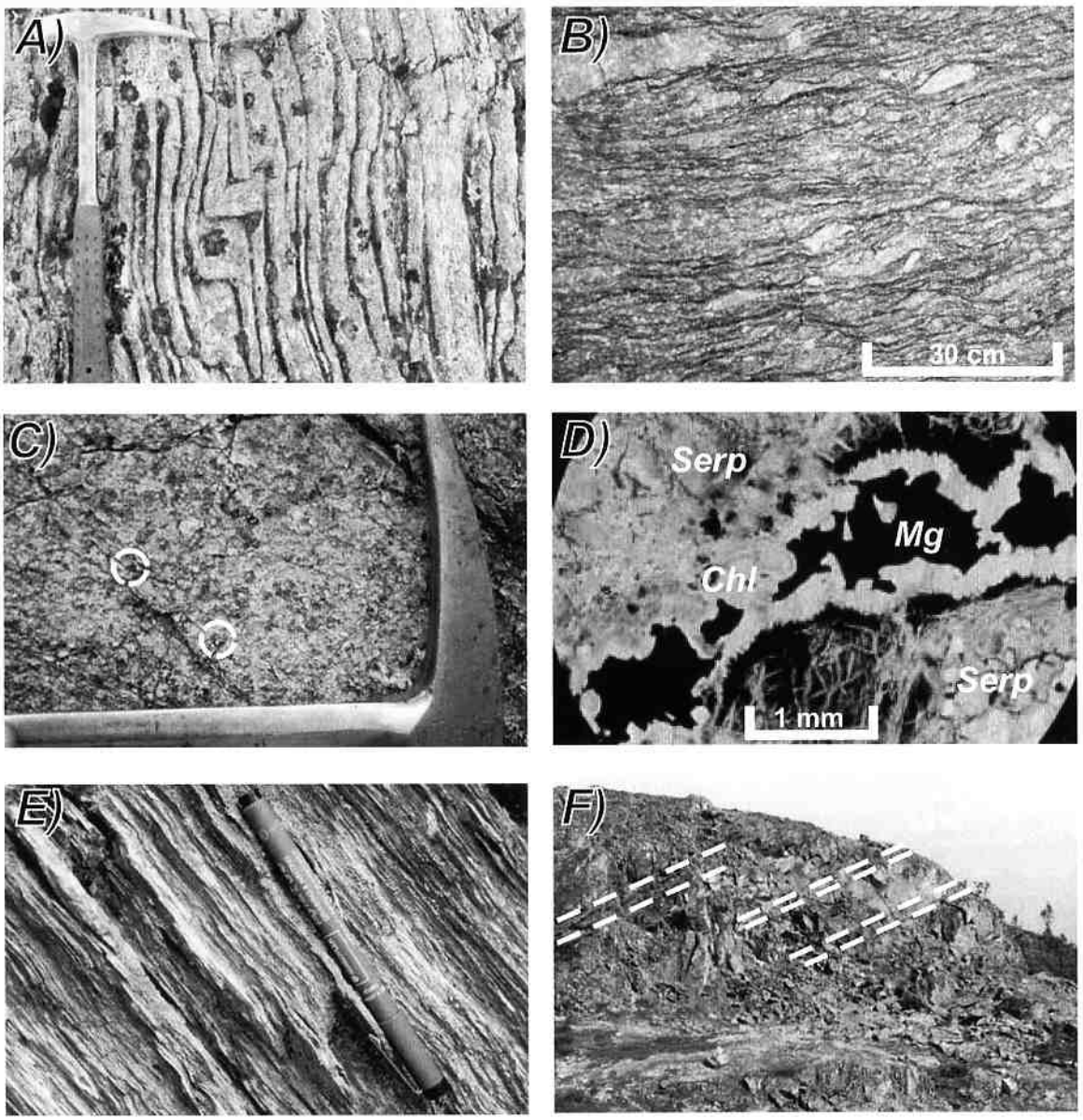

Figure 2.5: (A) Light bands of quartzite intercalated with thin bands of chlorite schist from the Pelmac Formation. (B) Basal quartzite-pebble to -cobble conglomerate from the Little Salmon Formation. (C) Raised dark spots (circled) in serpentinite represent serpentine pseudomorphs after pyroxene. (D) Photomicrograph of holly-leaf texture in serpentinite from the Tummel fault zone. Magnetite (Mg; after spinel) is surrounded by a halo of chlorite (Chl; after plagioclase). (E) A phyllonite outcrop marks a west-dipping thrust fault that indicates a component of ductile deformation in the evolution of the Tummel fault zone. (F) Thick sills of granite separated by thin layers of quartz-mica schist dip moderately to the southwest, suggesting an overall sheetlike geometry of the batholith.

clear, pale yellow, stubby prismatic zircon grains with simple terminations, rare clear bubble- and tube-shaped inclusions and no visible zoning or cores. Five strongly abraded fractions were analyzed (Table 2.2; Fig. 2.6A). All five analyses were concordant. Fractions A, C and D yield overlapping analyses with a total range of $^{206}Pb/^{238}U$ ages of 348.3 ± 1.1 Ma, which gives the crystallization age of the sample. The remaining two fractions (B and E) yield slightly younger $^{206}Pb/^{238}U$ ages, presumably reflecting the effects of minor post-crystallization Pb-loss.

Similar U-Pb zircon ages of 348-349 Ma were obtained from samples of foliated hornblende-biotite quartz diorite and tonalite that intrudes rocks of the Snowcap Complex and Pelmac Formation at Telegraph Mountain on the western border of Truitt Creek map area (Fig. 2.1; Colpron et al., in review-a). These are the oldest plutons of the Little Kalzas plutonic suite. To the north, the Little Kalzas plutonic suite is the most extensive suite of magmatic rocks in Yukon-Tanana terrane, with crystallization ages of most plutons clustering at ca. 347-345 Ma (Colpron et al., in review-a).

Little Salmon Formation

The Little Salmon Formation is a sequence of volcaniclastic rocks, andesite, and basalt of middle Mississippian to Pennsylvanian age, primarily exposed north of Little Salmon Lake (Fig. 2.1; Colpron et al., in review-a). The Little Salmon Formation conformably overlies the Pelmac Formation to the west and the Drury Formation to the east. In Truitt Creek map area, the Little Salmon Formation occurs in a narrow northwest-trending belt in the western central part of the map area (Fig. 2.2), and includes conglomerate, marble, and intermediate volcaniclastic rocks. The base of the succession

Sample Description[1]	Wt (mg)	U (ppm)	Pb^2 (ppm)	$^{206}Pb/^{204}Pb$ (meas.)[3]	total common Pb (pg)	% $^{208}Pb^2$	$^{206}Pb/^{238}U^4$ (± % 1s)	$^{207}Pb/^{235}U^4$ (± % 1s)	$^{207}Pb/^{206}Pb^4$ (± % 1s)	$^{206}Pb/^{238}U$ age (Ma; ± % 2 s)	$^{207}Pb/^{206}Pb$ age (Ma; ± % 2s)
Sample KG01-220											
A: N2, +149	0.047	193	10.8	5157	6	10.4	0.05552(0.16)	0.4087(0.28)	0.05339(0.23)	348.3(1.1)	345.4(10.3)
B: N2, +149	0.050	215	11.9	6957	5	10.1	0.05500(0.10)	0.4058(0.22)	0.05351(0.16)	345.1(0.7)	350.7(7.3)
C: N2, +149	0.047	214	12.1	7884	4	10.7	0.05558(0.09)	0.4099(0.20)	0.05348(0.15)	348.7(0.6)	349.3(6.9)
D: N2, +149	0.067	199	11.2	9259	5	10.6	0.05557(0.12)	0.4093(0.21)	0.05342(0.15)	348.6(0.8)	346.5(6.6)
E: +149	0.072	285	15.8	13080	5	9.7	0.05516(0.11)	0.4076(0.18)	0.05359(0.11)	346.1(0.7)	353.9(5.0)
Sample 99MC-034											
A: N2,+134	0.030	158	8.4	3027	5	7.8	0.05386(0.11)	0.4056(0.19)	0.05462(0.12)	338.2(0.8)	396.8(5.3)
B: N2,+134	0.030	243	19.9	8411	4	13.1	0.07589(0.11)	0.9216(0.17)	0.08808(0.09)	471.5(1.0)	1384.3(3.3)
D: N2,+134	0.031	77	4.3	2036	4	8.6	0.05618(0.13)	0.4426(0.22)	0.05714(0.14)	352.3(0.9)	496.9(6.1)
E: N2,+134	0.022	315	17.0	2525	9	8.2	0.05447(0.11)	0.4077(0.20)	0.05428(0.12)	341.9(0.7)	382.5(5.4)
Sample KG02-048											
A: N10,+134	0.021	70	3.2	2954	1	15.7	0.04218(0.23)	0.2998(0.59)	0.05155(0.53)	266.3(1.2)	165.6(24.3)
C: N10,+134	0.017	167	7.6	4066	2	16.8	0.04198(0.13)	0.3001(0.19)	0.05185(0.13)	265.1(0.7)	278.7(5.9)
D: N10,+134	0.017	205	9.4	1953	5	17.4	0.04194(0.15)	0.2977(0.56)	0.05149(0.52)	264.9(0.8)	262.6(23.7)
E: N10,+134	0.009	45	2.0	497	2	15.1	0.04241(0.29)	0.3004(2.02)	0.05138(1.91)	267.8(1.5)	257.9(87.2)
Sample KG01-188											
A: N10,74-92	0.011	1407	20.9	1126	14	2.1	0.01616(0.12)	0.1077(0.92)	0.04834(0.87)	103.3(0.2)	116.1(41.2)
B: N10,74-92	0.008	322	8.3	1311	3	6.0	0.02631(0.26)	0.2443(0.65)	0.06735(0.58)	167.4(0.9)	848.7(24.2)
C: N10,44-74	0.010	2367	38.5	608	40	8.9	0.01636(0.16)	0.1191(1.56)	0.05278(1.50)	104.6(0.3)	319.4(67.9)
D: N10, 44-74	0.007	922	17.9	733	13	25.9	0.01592(0.13)	0.1055(1.07)	0.04807(1.02)	101.8(0.3)	102.9(48.1)

Notes: [1] N2,N10 = non-magnetic at n degrees side slope on Frantz magnetic separator; grain size given in microns.
[2] radiogenic Pb; corrected for blank, initial common Pb, and spike. [3] corrected for spike and fractionation. [4] corrected for blank Pb and U, and common Pb.

Table 2.2: U-Pb analytical data for four samples from Truitt Creek map area. (Ages and locations of samples shown in Fig. 2.2).

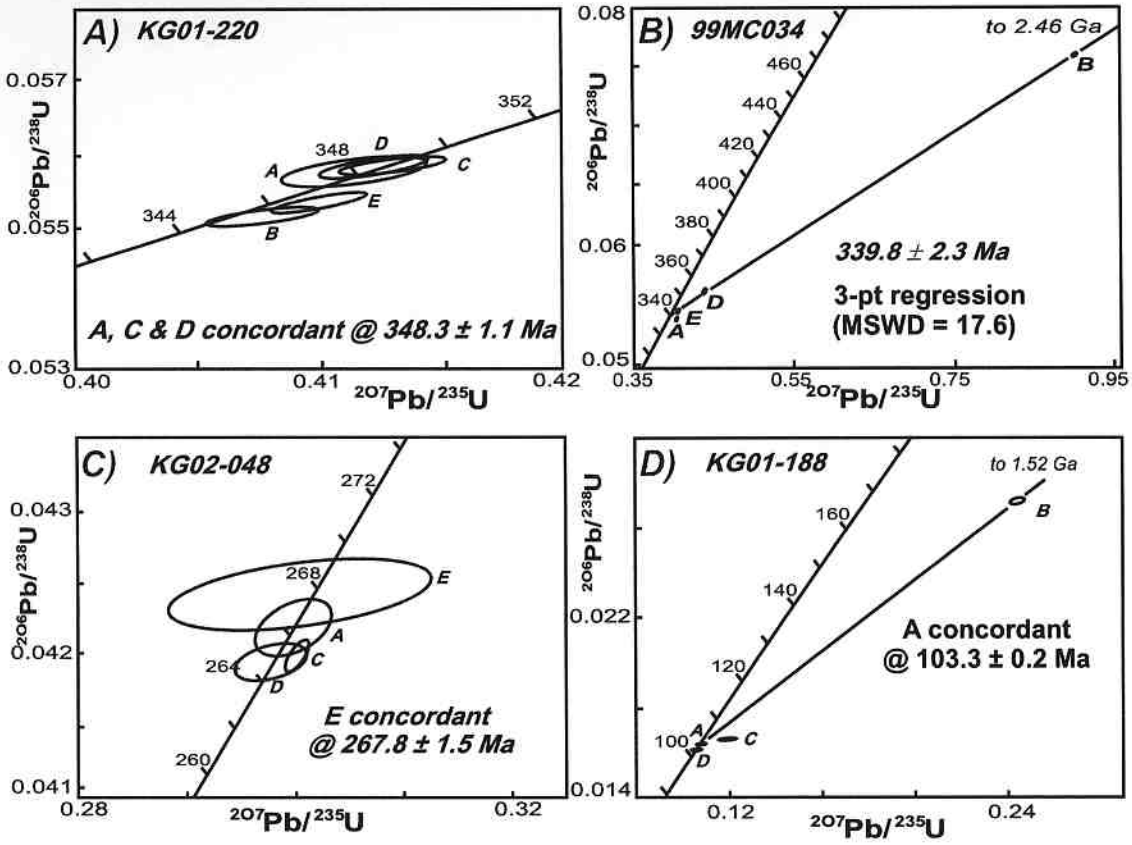

Figure 2.6: U-Pb concordia diagrams: (A) Hornblende granodiorite sample KG01-220 of the Little Kalzas suite. (B) Granodiorite sample 99MC034 taken along Robert Campbell Highway. (C) Basalt sample KG02-048 from the Tummel fault zone. (D) Hornblende leucogabbro sample KG01-188 from the Tummel fault zone. (Ages and locations of samples shown on Fig. 2.2).

is an unconformity marked by a quartzite-pebble to -boulder conglomerate which has subangular to subrounded clasts of grey quartzite supported by a green-grey chloritic matrix (Fig. 2.5B). Tightly folded fabric observed within some of the boulders indicates derivation from a deformed and metamorphosed source terrane.

Locally, a phlogopite-bearing marble conformably overlies the lower conglomerate member of the Little Salmon Formation (Fig. 2.2). This marble is correlated with marble north of Little Salmon Lake that contains late Viséan-Moscovian (Late Mississippian — middle Pennsylvanian) corals (E.W. Bamber *in* Colpron and Reinecke, 2000). Chlorite + epidote ± biotite ± magnetite schist is the uppermost member of the Little Salmon Formation. The schist lies conformably above the marble unit, and is preserved as keels in gentle synformal folds of regional foliation (Fig. 2.2).

A sample of quartz-feldspar porphyry from the base of the Little Salmon Formation north of Little Salmon Lake has yielded a concordant U-Pb zircon age of 340.2 Ma (Colpron et al., in review), providing a maximum age of the Little Salmon sequence.

Zircon recovered from a sample of granodiorite taken from a pluton along Robert Campbell Highway (Fig. 2.2) comprised stubby, pale pink, multifaceted prisms. Four strongly abraded fractions yield scattered analyses with Pb/Pb ages up to 1384 Ma (Table 2.2; Fig. 2.6B). Three of the analyses (B, D and E) define a linear array with calculated lower and upper intercept ages of 339.8 ± 2.3 Ma and 2.46 Ga, respectively. The lower intercept is considered to be the best estimate for the crystallization age of the sample and the upper intercept indicates mainly Paleoproterozoic inherited cores were present in many of the grains. The fourth fraction (A) appears to have contained a minor older inherited component and to have suffered minor post-crystallization Pb-loss effects that

were not completely removed by the strong abrasion. This pluton is interpreted as part of the plutonic root of the Little Salmon magmatic arc system.

Summary of Yukon-Tanana evolution recorded in Truitt Creek area

Yukon-Tanana terrane in Truitt Creek area consists of pre-Upper Devonian quartzofeldspathic basement rocks of the Snowcap Complex that are overlain by Mississippian siliciclastic and volcanic rocks of the Drury and Pelmac formations, whose sediments are derived in part from Snowcap-equivalent rocks. The ca. 343-349 Ma Little Kalzas magmatic arc sits above the Pelmac Formation, and its plutonic equivalent intrudes the older Yukon-Tanana components. Volcanic rocks of the Little Salmon Formation record a second pulse of arc-related magmatism. The rocks of Yukon-Tanana terrane have a well-developed schistosity that has overprinted and obscured primary layering in most exposures. Based on cross-sections, we estimate that a total thickness of 5-6 km of Devonian-Mississippian Yukon-Tanana terrane stratigraphy is present (Fig. 2.2).

Tummel fault zone

The Tummel fault zone is a narrow band, ca. 100 km long and up to 3 km wide, that is characterized by lithologies unlike those of Cassiar terrane to the northeast or Yukon-Tanana terrane to the southwest. Central and northwestern sections of the zone are underlain by fine-grained, foliated, moderately to highly altered, light and dark green basalt and greenstone, commonly with relict plagioclase and clinopyroxene phenocrysts. Clinopyroxene phenocrysts and plagioclase twinning are locally preserved, but most

greenstones are more highly altered and contain significant amounts of epidote, chlorite, calcite, and serpentine.

At the southeastern end of the Tummel fault zone, and along Robert Campbell Highway, chert is the dominant lithology, with lesser quartzite, micaceous quartzite, and locally graphitic black slate. At the highway, the chert is pale green and massive, with 7-8 mm wide pyrite porphyroblasts. The chert is massive and black and white in the southeast, where an east-verging thrust fault places greenstone over chert (Fig. 2.5E). North of Drury Lake, chert depositionally overlies basalt (Colpron et al., 2003a).

Seven samples of metabasalt from the Tummel fault zone were analyzed for major and trace elements (Table 2.1). Discrimination diagrams show that all these rocks are subalkaline basalt, with trace element signatures that suggest MORB character (Fig. 2.4). Primitive mantle-normalized multi-element plots of trace element concentrations reveals two groups: four samples with flat profiles (Fig. 2.3C) contrast with three samples characterized by significant Nb-depletion (Fig. 2.3D). The intercalated Nb-depleted and non-depleted basalts suggests proximity to an arc environment during formation. Four strongly abraded fractions of clear, colorless, euhedral, multifaceted stubby prismatic zircons from a sample of basalt taken near the centre of the map area were analyzed (KG02-048; Fig. 2.2). All yielded concordant analyses (Table 2.2; Fig. 2.6C). Fraction E gives the oldest $^{206}Pb/^{238}U$ ages of 267.8 ± 1.5 Ma, which is interpreted as the crystallization age of the sample. The other three fractions have suffered minor post-crystallization Pb-loss.

Coarse-grained serpentinized harzburgite occurs in several places within the Tummel fault zone, most notably in an elongate, northwest-trending exposure in the central part of

the map area (Fig. 2.2). Contacts between harzburgite and adjacent greenstone are not exposed. A black and white, medium-grained, altered hornblende-chlorite-saussurite mylonite occurs 100 m northeast of the same exposure, with a steeply (84°) south-southwest-dipping fabric that projects beneath the harzburgite.

Quartz-carbonate and antigorite veins <1 cm thick cut the harzburgite. White crystals of carbonate with a radiating habit, 1-3 mm in diameter, commonly give the rock a distinctive speckled appearance. Serpentine pseudomorphs after orthopyroxene crystals 4-6 mm wide characterize the peridotite (Fig. 2.5C), and are locally strung out over distances of >30 cm. Primary spinel with plagioclase coronae have been replaced by holly leaf magnetite and chlorite pseudomorphs, respectively (Fig. 2.5D).

The holly-leaf shape of magnetite (originally spinel) crystals observed in thin section (Fig. 2.5D) and the coarse grain size and strung-out texture of the orthopyroxene porphyroclasts indicate recrystallization and solid-state deformation at mantle temperatures (~1250° C; Nicolas, 1995). Thus, petrographic observations, together with fabric relationships in harzburgite and surrounding rocks, indicate that the harzburgite originated as mantle tectonite, and was structurally emplaced in the Tummel fault zone.

A gabbro klippe above Cassiar terrane strata near Ragged Lake (Fig. 2.1) has yielded a 260 Ma U-Pb zircon date (Colpron et al., in review-a). Its mafic composition, age, and position along strike to the northwest suggest that it is correlative with Tummel fault zone rocks. A sample from a deformed granite dyke within the Dunite klippe to the south of the study area (Fig. 2.1) has yielded a concordant U-Pb zircon age of 267 ± 10 Ma (de Keijzer et al., 1999b) and may also be related to the Permian basalts preserved in the Tummel fault zone.

The association of basalt, chert, and harzburgite in the Tummel fault zone resembles the Campbell Range succession of the Finlayson Lake area in southeastern Yukon (Colpron et al., 2003b; Murphy et al., 2001) and the Sylvester allochthon of northern British Columbia (Nelson, 1993), although the 267 Ma age of the Tummel fault zone basalt is somewhat younger than radiometric ages typically reported from Slide Mountain.

Mid-Cretaceous intrusions

Glenlyon Batholith is a composite, multi-phase intrusion that is part of the Anvil-Cassiar plutonic suite, which is widespread in southeastern Yukon and northeastern British Columbia (Woodsworth et al., 1991). Glenlyon Batholith is well exposed to the east of the Tummel fault zone, where it intrudes the Kechika and Askin groups (Fig. 2.2). Three intrusive phases are present in the batholith: (1) early medium-grained hornblende-biotite granodiorite, intruded by (2) voluminous medium- to coarse-grained, locally plagioclase- or potassium feldspar-porphyritic, biotite ± muscovite granite, cut by (3) late muscovite-quartz-plagioclase pegmatite dykes. Five andesite dykes, 1-5 m wide, cut the batholith.

The batholith margins are characterized by lit-par-lit gneiss that dips gently to moderately (~30°) to the southwest, parallel to foliation in the enclosing schist (Fig. 2.5F); this suggests that the gross geometry of the batholith is a sheet-like body or series of bodies. Pendants of quartz + muscovite + biotite ± garnet schist ranging from tens to hundreds of metres across are common within the intrusion at topographic high points and near the batholith margin. This may indicate that the present level of exposure is near

the roof of the batholith. A weak foliation of aligned phenocrysts, interpreted as a magmatic feature, is locally present in the intrusion.

The age of Glenlyon Batholith is not well constrained in the study area. Whole rock K-Ar analysis of hornfels adjacent to the Glenlyon batholith on the north side of the highway has yielded a cooling age of 105 ± 4 Ma (Fig. 2.2; Hunt and Roddick, 1990). A sample of biotite-hornblende quartz diorite taken 10 km east of the study area yielded a K-Ar hornblende cooling age of 102.7 ± 2.3 Ma (Fig. 2.2; Hunt and Roddick, 1991). A hornblende porphyry dyke north of the study area gave a slightly younger Ar-Ar biotite cooling age of 95.6 ± 1.0 Ma (Hunt and Roddick, 1992). A U-Pb zircon age of 108.1 ± 0.2 Ma was obtained from quartz-feldspar porphyry encountered in drill core at the Clear Lake deposit approximately 70 km to the north (Breitsprecher et al., 2002). A similar age of 109 ± 3 Ma was obtained from U-Pb monazite analysis of a sample from the d'Abbadie pluton, 15 km to the south in Laberge map area (de Keijzer, 2000), which is lithologically similar to and is continuous with Glenlyon Batholith (Fig. 2.1). Thus, an age of 109-96 Ma is indicated for Glenlyon Batholith, based on and consistent with cooling ages reported from the batholith and its aureole.

A pluton of medium- to coarse-grained hornblende leucogabbro intrudes greenstone within the central part of the Tummel fault zone (Fig. 2.2). Xenoliths of foliated greenstone are found within the leucogabbro, and chilled margins were noted at intrusive contacts. Smaller intrusions and dykes of leucogabbro and hornblende ± biotite diorite were observed elsewhere in the Tummel fault zone. These intrusions have a weak to moderate magmatic foliation defined by margin-parallel alignment of hornblende grains that truncates the dominant schistosity in the greenstone. A sample of hornblende

leucogabbro from the Tummel fault zone pluton yielded a very small amount of square, pale brown, stubby to prismatic zircon grains. All grains >44 microns in diameter were subjected to moderate abrasion prior to dissolution. Two of the resulting analyses (A and D; Table 2.2, Fig. 2.6D) are concordant, and two are moderately to strongly discordant with considerably older Pb/Pb ages, indicating the presence of older inherited zircon components. The zircons contained moderate to high concentrations of U (up to 2367 ppm), and it is likely that some or all of the fractions have suffered at least some post-crystallization Pb-loss. The $^{206}Pb/^{238}U$ ages of 103.3 ± 1.5 Ma for fraction A is interpreted to be a minimum estimate for the emplacement age of this body, and the calculated upper intercept age of 1.52 Ga for a two-point regression through fraction A and the most discordant fraction (B) indicates mainly Mesozoproterozoic inheritance. Fraction D evidently contained no inherited zircon component but had experienced Pb-loss, and fraction C contained minor inheritance and also experienced Pb-loss. Based on their spatial association and similar ages, we interpret the leucogabbro as a mafic phase of the Anvil-Cassiar plutonic suite.

Structure and metamorphism

The style and history of deformation and metamorphism vary across the map area. In Cassiar terrane, a southwest-dipping phyllitic foliation along the Robert Campbell Highway is overprinted by a well-developed southwest-dipping schistosity near the Glenlyon Batholith in the southeast part of the map area. Compositional layering is commonly parallel to foliation, and a moderately southwest-plunging crenulation lineation is locally developed. East of Little Salmon Lake and adjacent to the Tummel

fault zone in the southeast part of the map area, pelitic and overlying carbonate strata are folded into kilometre-scale, north-northwest-trending open synclines (Fig. 2.2). Stratigraphy in the southeast corner of the map area has been dextrally offset 1 km by a northeast-trending subvertical strike-slip fault.

Chlorite and muscovite in phyllite of the Kechika Group at the Robert Campbell highway indicate that these rocks have experienced low-grade regional metamorphism. Younger metamorphic features associated with emplacement of Glenlyon Batholith (discussed below) overprint the phyllitic foliation.

Southwest of the Tummel fault zone, a polyphase deformational history is recorded in rocks of Yukon-Tanana terrane. The dominant foliation in Yukon-Tanana rocks is a moderate to strongly developed schistosity that is folded into broad northwest-trending kilometer-scale folds (Fig. 2.2). Primary layering observed in Mississippian rocks parallels schistosity. Mineral parageneses in rocks of Yukon-Tanana terrane indicate middle to upper greenschist facies metamorphism (chlorite- to garnet-grade). Early Jurassic $^{40}Ar/^{39}Ar$ white mica cooling ages from samples collected along Little Salmon Lake (Oliver, 1996) indicate that regional metamorphism occurred prior to Early Jurassic time. The Snowcap Complex has undergone at least one deformational event that is not recognized in overlying Mississippian units (Colpron et al., in review-a).

Permian greenstone and chert within the Tummel fault zone has a dominant northwest-trending S_2 schistosity that is axial planar to isoclinal folds of an earlier S_1 schistosity. A moderately to steeply east-dipping spaced crenulation cleavage (S_3) is commonly developed. The epidote + actinolite + chlorite + plagioclase mineral assemblage that characterizes the metabasalt indicates that these rocks have reached

middle greenschist facies metamorphic conditions. An intensely fractured cataclastic texture that locally overprints fabric in greenstone and chert indicates a component of post-metamorphic brittle deformation which is not found in adjacent terranes.

Regional greenschist facies metamorphism recorded in chlorite-grade phyllite exposed in the Magundy reentrant is overprinted by a higher-grade contact metamorphic aureole adjacent to Glenlyon Batholith. Near the batholith margins, well-developed schistosity dips consistently shallowly to the west, parallel to compositional layering and to intrusive contacts. Metamorphic grade decreases away from the batholith to the southwest (Gladwin et al., 2003; Gordey and Makepeace, 2000).

Microprobe analysis of metamorphic mineral parageneses in wall rocks adjacent to Glenlyon Batholith in the southeastern part of Truitt Creek map area was used to estimate pressure and temperature conditions at the time of intrusion (Black, 2002). Samples of metapelite with garnet + biotite + quartz + muscovite + plagioclase ± cordierite ± andalusite, and calc-silicate rocks with garnet + clinopyroxene + quartz mineral parageneses were selected for analyses.

Geothermobarometry results and oxide data from microprobe analyses are summarized in Tables 2.3 and 2.4, respectively. A pressure estimate of 3.1 kbar was calculated from a garnet-mica-aluminosilicate assemblage (KG01-155; Fig. 2.7A). A temperature of 590° C was calculated from a garnet-diopside assemblage (RB01-004; Fig. 2.7B). Garnet-biotite geothermometers from two samples (KG01-155 and RB02-012; Fig. 2.7A,C) returned calculated values of 740° C and 730° C, respectively, which are too high to be consistent with the presence of muscovite + andalusite + quartz in the samples, and with peak metamorphic conditions of lower amphibolite facies indicated by

Sample[1]	Rock name	Mineralogy	Thermometer/ barometer used	Calc. T (°C) at 3 kbar	Calc. P (kPa)
KG01-155	garnet-biotite-muscovite schist	quartz, muscovite, biotite, almandine, albite, andalusite, tourmaline	garnet-mica-aluminosilicate, garnet-biotite	740	3.1
RB01-004	garnet-calc-silicate schist	almandine, diopside, calcite, titanite, epidote, plagioclase	garnet-diopside	590	-
RB02-012	garnet-biotite-muscovite schist	quartz, almandine, muscovite, biotite, albite, chlorite	garnet-biotite	730	-

[1]*Sample locations indicated in Figure 2.2.*

Table 2.3: Geothermobarometry results from country rock samples adjacent to Glenlyon Batholith.

Sample **RB01-004**

Garnet	Na	Mg	Al	Si	Ca	Ti	Cr	Mn	Fe	total
004-1	0.037	1.535	21.394	36.523	9.633	0.141	0.008	0.658	29.091	99.02
004-2	0.030	1.160	21.426	37.106	9.926	0.172	0.000	0.803	29.551	100.18
004-3	0.026	1.029	21.330	36.798	9.995	0.139	0.045	1.274	29.041	99.68
004-4	0.046	1.103	21.544	37.103	9.784	0.144	0.022	1.156	29.855	100.76

Pyroxene	Na	Mg	Al	Si	Ca	Ti	Cr	Mn	Fe	total
004-1	0.076	8.614	0.368	51.200	23.571	0.000	0.021	0.224	14.985	99.06
004-2	0.085	9.216	0.326	51.053	23.709	0.002	0.013	0.273	14.986	99.66
004-3	0.078	9.429	0.250	51.520	23.402	0.035	0.019	0.303	14.420	99.46
004-4	0.093	9.469	0.221	51.247	23.313	0.014	0.021	0.310	14.298	98.99

Sample **RB02-012**

Garnet	Na	Mg	Al	Si	Ca	Ti	Cr	Mn	Fe	total
012-1	0.027	2.369	21.581	37.041	7.121	0.094	0.039	0.304	31.640	100.22
012-2	0.012	1.851	21.411	37.122	7.153	0.074	0.000	0.276	32.399	100.30
012-3	0.040	1.192	21.068	36.893	8.302	0.090	0.014	1.927	30.682	100.21
012-4	0.007	1.106	21.247	36.773	8.719	0.110	0.014	2.527	29.897	100.40
012-7	0.004	2.119	21.661	36.977	6.438	0.083	0.023	0.253	32.904	100.46
012-8	0.016	1.628	21.267	36.868	6.990	0.044	0.040	0.543	32.536	99.93
012-9	0.042	1.116	21.241	37.048	8.770	0.108	0.002	2.387	29.958	100.67
012-10	0.007	1.363	21.457	36.958	7.973	0.090	0.000	0.953	31.357	100.16

Biotite	Na	Mg	Al	Si	K	Ca	Ti	Cr	Mn	Fe	Ba	F	Cl	total
012-1	0.235	7.672	19.208	35.844	9.632	0.027	2.795	0.000	0.075	20.462	0.042	0.254	0.000	95.99
012-2	0.163	7.779	19.383	35.977	9.829	0.000	2.823	0.038	0.061	20.675	0.052	0.311	0.013	96.78
012-5	0.238	8.556	18.614	35.755	9.649	0.000	2.984	0.026	0.078	20.241	0.114	0.340	0.045	96.26
012-6	0.229	8.742	18.378	36.545	9.636	0.000	2.952	0.046	0.070	19.455	0.019	0.400	0.000	96.07
012-9	0.144	5.761	18.870	34.820	9.482	0.003	3.218	0.071	0.122	23.746	0.108	0.108	0.000	96.34
012-10	0.131	5.639	19.210	34.753	9.667	0.001	3.221	0.058	0.160	23.475	0.085	0.210	0.034	96.40

Feldspar	Na	Mg	Al	Si	K	Ca	Fe	total
012-3	6.091	0.000	27.416	57.620	0.261	9.372	0.033	100.79
012-4	5.806	0.011	27.859	56.359	0.243	9.960	0.046	100.28

White Mica	Na	Mg	Al	Si	K	Ca	Ti	Cr	Mn	Fe	Ba	F	Cl	total
012-3	0.440	1.181	33.541	47.516	10.256	0.010	0.740	0.032	0.009	1.613	0.212	0.130	0.008	95.55
012-4	0.410	1.003	33.412	46.519	9.782	0.020	0.560	0.013	0.000	1.238	0.261	0.143	0.039	93.22
012-7	0.462	0.869	34.844	45.904	10.529	0.000	0.486	0.043	0.072	1.486	0.313	0.063	0.000	95.01
012-8	0.501	1.211	33.537	46.712	10.568	0.006	0.524	0.041	0.000	1.519	0.217	0.153	0.011	94.84

Sample **KG01-155**

Garnet	Na	Mg	Al	Si	Ca	Ti	Cr	Mn	Fe	total
155-1	0.003	1.516	21.465	36.548	8.802	0.086	0.074	0.635	30.701	99.83
155-2	0.008	1.282	21.425	36.882	9.234	0.106	0.000	0.800	30.420	100.16
155-3	0.011	1.310	21.440	36.473	8.925	0.120	0.000	0.751	30.445	99.48
155-4	0.016	1.224	21.398	37.053	9.331	0.083	0.006	0.836	29.888	99.83
155-5	0.044	0.993	21.533	36.873	9.274	0.109	0.029	2.685	28.548	100.09
155-6	0.031	0.970	21.297	36.622	9.543	0.128	0.014	2.877	28.089	99.57

Biotite	Na	Mg	Al	Si	K	Ca	Ti	Cr	Mn	Fe	Ba	F	Cl	total
155-1	0.153	7.526	17.336	35.123	9.403	0.047	2.500	0.072	0.215	23.294	0.180	0.475	0.102	95.85
155-2	0.135	7.514	17.470	34.806	9.193	0.068	2.393	0.072	0.193	23.562	0.197	0.473	0.181	95.60
155-4	0.051	9.052	18.099	32.493	6.363	0.076	1.442	0.010	0.263	25.540	0.115	0.332	0.149	93.50
155-6	0.183	8.450	19.230	36.134	9.873	0.002	2.431	0.062	0.218	20.037	0.122	0.450	0.076	96.74
155-7	0.122	8.446	19.202	36.111	9.874	0.001	2.341	0.000	0.180	20.100	0.096	0.429	0.065	96.47
155-10	0.053	6.324	20.897	33.200	8.808	0.052	0.687	0.028	0.190	24.468	0.032	0.237	0.132	94.74

Feldspar	Na	Mg	Al	Si	K	Ca	Fe	total
155-1	5.520	0.002	28.466	55.790	0.097	10.518	0.322	100.72
155-2	6.168	0.000	27.204	57.328	0.144	9.063	0.075	99.98
155-3	5.772	0.000	27.631	56.198	0.142	9.930	0.098	99.77

White Mica	Na	Mg	Al	Si	K	Ca	Ti	Cr	Mn	Fe	Ba	F	Cl	total
155-8	0.405	0.044	18.455	65.474	16.267	0.000	0.021	0.015	0.000	0.247	0.275	0.001	0.008	101.20
155-9	0.399	0.027	18.496	65.773	16.430	0.020	0.000	0.002	0.038	0.409	0.155	0.001	0.000	101.75

Table 2.4: Oxide percent data by mineral from electron microprobe analyses. Data was reduced using TWEEQU software (after Berman, 1991).

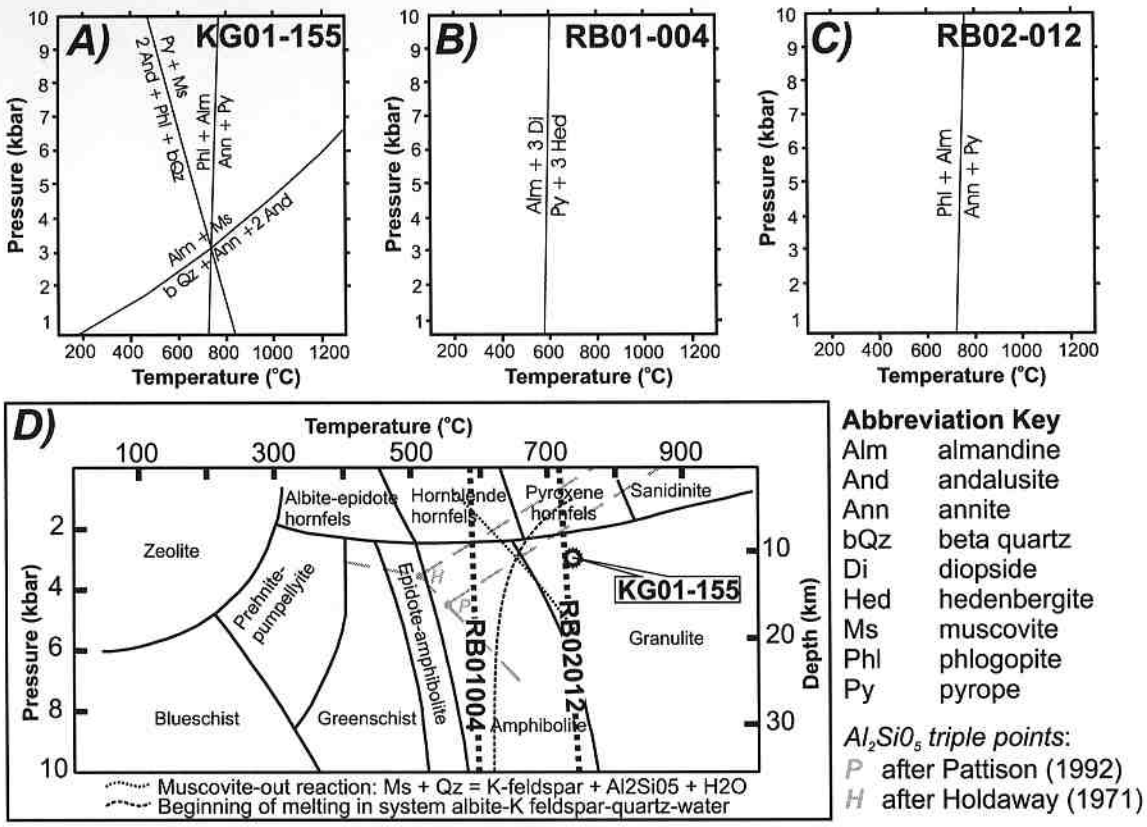

Figure 2.7: Geothermometry and geobarometry diagrams: (A) Sample KG01-155. (B) Sample RB01-004. (C) Sample RB02-012. (D) Samples plotted in P-T space are broadly consistent with lower amphibolite facies metamorphic conditions.

mineral parageneses observed in surrounding rocks. Errors on values reported here are ±50°C on the garnet-biotite geothermometer (Ferry and Spear, 1978) and ±800 bars on the garnet-mica-aluminosilicate geobarometer (Ghent and Stout, 1981). These are minimum error estimates reported in the respective original experimental work, and do not include errors in the calculated temperature compounded by error associated with the geobarometer, or analytical error on microprobe results. However, pressure conditions of 3.1 kbar and a temperature of 590° C during emplacement of the Glenlyon Batholith are consistent with lower amphibolite facies metamorphism indicated by mineral parageneses in cordierite- and andalusite-bearing country rock (Fig. 2.7D).

The Glenlyon-imposed contact metamorphic aureole extends >5 km to the southwest, across the Tummel fault zone and into the Drury Formation of Yukon-Tanana terrane, where cordierite, andalusite, and garnet porphyroblasts overgrow the dominant foliation. In the Tummel fault zone, andalusite and garnet porphyroblasts locally overprint dominant foliation in the chert-dominated unit. In the southeast part of the map area, geothermobarometric data from biotite-garnet schist adjacent to the intrusion indicates that lower amphibolite facies conditions were reached during intrusion (Fig. 2.7D). Because Glenlyon-related contact metamorphism is recorded in all three tectonic assemblages in the Truitt Creek map area, juxtaposition of these assemblages must predate intrusion of the batholith, consistent with satellite plutons of the batholith that intrude the Tummel fault zone.

Discussion

Mapping of Truitt Creek area shows that Devonian to Mississippian continental margin and arc rocks of Yukon-Tanana terrane are juxtaposed against continental margin strata of Cassiar terrane along the Tummel fault zone.

Cassiar terrane records Lower Paleozoic miogeoclinal sedimentation that evolved from a clastic-dominated basin up into a carbonate platform setting. This contrasts with Yukon-Tanana terrane, where pre-Upper Devonian to Mississippian coarse siliciclastic sedimentation gives way to a Lower Mississippian continental arc setting that preserves two magmatic events (Colpron et al., in review-a). A Permian ocean basin setting is preserved in the basalt, chert, and ultramafic rocks of the Tummel fault zone.

Geochemical signatures reveal further contrasts among the three tectonic assemblages. Within-plate alkalic mafic magmatism is recorded by amphibolite samples from Cassiar terrane. In Yukon-Tanana terrane, both the ca. 343-349 Ma Little Kalzas and the ca. 340 Ma Little Salmon formations include calc-alkaline andesite and alkali basalt that represent continental arc magmatism evolving into a rifted arc setting (Colpron, 2001). Permian basalt and greenstone from the Tummel fault zone have a geochemical signal with mixed MORB and island arc tholeiite components, suggesting a tectonic environment transitional between a marginal basin and arc setting.

Chlorite-grade regional metamorphism of Cassiar terrane is overprinted by higher grade contact metamorphism associated with the Glenlyon Batholith. In Yukon-Tanana terrane, a regional biotite- to garnet-grade metamorphic event produced schistosity that has since been folded and overprinted by the Glenlyon contact aureole. An early schistosity in metabasalt of the Tummel fault zone was transposed into parallelism with

the dominant schistosity; these early fabrics are overprinted by a late crenulation cleavage, brittle deformation, and Glenlyon Batholith-related, retrogressive contact metamorphism.

Contrasting stratigraphy, geochemistry, and structural and metamorphic history support the conclusion that Yukon-Tanana terrane is exotic with respect to Cassiar terrane. A post-267 Ma (age of basalt within the Tummel fault zone) but pre-105 Ma (age of satellite intrusions of Glenlyon batholith within the Tummel fault zone) time of juxtaposition is indicated. Synorogenic Permian-Triassic conglomerate along strike to the northwest of this study was reported by Colpron et al. (2003a), and probably records juxtaposition of Yukon-Tanana and Cassiar terranes.

A paucity of marker units across the Tummel fault zone precludes a direct measurement of the nature and amount of displacement that it has accommodated. Because a mid-Cretaceous contact metamorphic aureole attributable to the Glenlyon Batholith extends from Cassiar terrane across the Tummel fault zone and into Yukon-Tanana terrane, these three tectonic entities must have been juxtaposed before ca. 105 Ma, and little displacement along the Tummel fault zone can have occurred since then.

Further south, in Laberge map area, stratigraphic offsets and detailed structural fabric analysis have been used to demonstrate that d'Abbadie fault (Fig. 2.1) is a late brittle structure that has accommodated ~4 km of dextral strike-slip displacement (de Keijzer et al., 1999a; Harvey et al., 1997). Timing of displacement on the d'Abbadie fault is constrained by the synkinematic Last Peak pluton (98 Ma, U-Pb monazite: Harvey et al., 1997) and by 96 Ma $^{40}Ar/^{39}Ar$ cooling dates from muscovite and biotite of the adjacent Mendocina orthogneiss (Hansen, 1992; Hansen et al., 1991). The cataclastic texture

common in chert and greenstone within the Tummel fault zone is not present in adjacent rocks of Yukon-Tanana or Cassiar terranes, and may be attributable to displacement on the order of that documented for the d'Abbadie fault.

At least one episode of crustal-scale faulting along the Tummel fault zone is indicated by the presence of mantle-derived ultramafic rocks. The association of harzburgite, basalt, greenstone, and chert in the Tummel fault zone suggest an ophiolitic origin, consistent with these rocks having originated in an ocean basin.

Eclogite occurrences in central Yukon record Early Permian high pressure, low temperature metamorphism (Erdmer et al., 1998). Metamorphic zircon from the Last Peak eclogite, 50 km south of the study area (Fig. 2.1) has been dated at 269 Ma (Creaser et al., 1997). Similar ages are reported from the St. Cyr klippe, 30 km east of Last Peak (267 Ma; Fallas, 1997), and from the Ross River and Faro eclogite occurrences (ca. 269 Ma; Erdmer et al., 1998). Low temperature, high pressure metamorphism indicated by the presence of eclogite may record nearby subduction during formation of oceanic rocks preserved in the Tummel fault zone.

Restoration of 425 km of Eocene dextral strike-slip displacement on Tintina fault (Murphy and Mortensen, 2003; Roddick, 1967) brings Cassiar terrane strata into continuity with strata of McEvoy platform northwest of the Tintina trench (Fig. 2.1A). The resultant elongate continental margin platform lies to the west of and shales out to the east into Selwyn Basin – Kechika Trough, a basinal region characterized by distal turbidites, shale, and chert. Thus, interpretation of Cassiar platform as part of the ancient North American margin requires that it be a high-standing block separated from the main

continental margin by Selwyn Basin – Kechika Trough, similar to Bahamas on the modern Atlantic passive margin.

Pope and Sears (1997) noted that the northern Cordillera is characterized by parallel archeocyathan-bearing belts: a westerly Cassiar platform belt, and an easterly belt in the carbonate platform of the ancient North American margin. They suggested that Cassiar platform is a displaced section of North American miogeocline that originated near present-day Idaho, where there is an absence of archeocyathan-bearing platform, and was transported northward to its present position. However, the outboard belt has been documented along much of the length of the North American Cordillera, and is not simply doubled up in Cassiar terrane in northern Canada (Fritz et al., 1991). Furthermore, this interpretation requires the eastern margin of Cassiar platform to be a fault that has accommodated large-scale translation, which is inconsistent with the present interpretation of that margin as a facies boundary (e.g. Gordey and Anderson, 1993; Wheeler and McFeely, 1991).

An exotic origin has also been suggested for Cassiar terrane. Paleomagnetic data from Late Cretaceous rocks across southern Yukon Territory, and from as nearby as Solitary Mountain (Fig. 2.1), requires that Cassiar platform and adjacent portions of Selwyn Basin were located 1750 ± 550 km to the south relative to cratonal North America at 70 Ma (Enkin et al., 2003). As well, Cassiar terrane has been correlated with coeval east-facing continental margin assemblages (the Nixon Fork terrane) that have been mapped into Alaska and that are characterized by Siberian, rather than North American, fauna (e.g. Johnston, 2001). However, geological mapping suggests that Cassiar terrane was tied to

cratonal North America by Paleozoic time, and structures capable of accommodating large-scale Late Cretaceous displacement relative to the craton have not been identified.

Summary

We have documented bedrock geology across the Tummel fault zone in Cassiar and Yukon-Tanana terranes in central Yukon Territory, and draw three important conclusions:

1.) Cassiar terrane records Paleozoic miogeoclinal sedimentation. Yukon-Tanana terrane consists of Mississippian arcs built upon Devonian-Mississippian siliciclastic basement. Permian ophiolitic assemblages with ocean basin and arc affinities are preserved in the Tummel fault zone.

2.) Contrasting stratigraphic, metamorphic, and deformational histories indicate that Yukon-Tanana and Cassiar terranes and Tummel fault zone rocks had separate early histories, and were tectonically juxtaposed.

3.) Intrusive and contact metamorphic features that extend across the Tummel fault zone record a shared history since at least mid-Cretaceous time. The Tummel fault zone probably records amalgamation of Cassiar and Yukon-Tanana terranes in Permian-Triassic time. Ophiolite along the fault separating the miogeoclinal Cassiar terrane from the accreted Yukon-Tanana terrane supports a model of continental growth by the closure of adjacent ocean basins and related terrane accretion.

References

Berman, R. G., 1991, Thermobarometry using multiequilibrium calculations: a new technique with petrologic applications: Canadian Mineralogist, v. 29, p. 833-855.

Berman, R. G., and Aranovich, L. Y., 1996, Optimized standard state and solution properties of minerals: I. Model calibration for olivine, orthopyroxene, cordierite, garnet, and ilmenite in the system FeO-MgO-CaO-Al_2O_3-TiO_2-SiO_2: Contributions to Mineralogy and Petrology, v. 126, no. 1-2, p. 1-24.

Berman, R. G., Aranovich, L. Y., and Pattison, D. R. M., 1995, Reassessment of the garnet-clinopyroxene Fe-Mg exchange thermometer: II, thermodynamic analysis: Contributions to Mineralogy and Petrology, v. 119, no. 1, p. 30-42.

Black, R., 2002, Geology and metamorphism of Cassiar terrane, Truitt Creek map sheet (105L/1), south-central Yukon [B.Sc. Honours thesis]: University of Victoria, 32 p.

Breitsprecher, K., Mortensen, J. K., and Villeneuve, M. E., 2002, YukonAge 2002: A database of isotopic age determinations for rock units from Yukon Territory, Canada, Exploration and Geological Services Division, Yukon Region, Indian and Northern Affairs Canada.

Campbell, R. G., 1967, Geology of Glenlyon map-area, Yukon Territory (105L), Geological Survey of Canada, 92 p.

Chatterjee, N. D., and Froese, E. F., 1975, A thermodynamic study of the pseudobinary join muscovite -paragonite in the system $KAlSi_3O_8$-$NaAlSi_3O_8$-Al_2O_3-SiO_2-H_2O: American Mineralogist, v. 60, p. 985-993.

Colpron, M., 2001, Geochemical characterization of Carboniferous volcanic successions from Yukon-Tanana terrane, Glenlyon map area (105L), central Yukon, *in* Emond, D. S., and Weston, L. H., eds., Yukon Exploration and Geology: Whitehorse, Yukon, Exploration and Geological Services Division, Yukon, Indian and Northern Affairs Canada, p. 111-136.

Colpron, M., Bond, J., Murphy, D. C., Nelson, J. L., Roots, C. F., Gladwin, K., Gordey, S. P., and Abbott, J. G., 2003a, Bedrock geology and till geochemistry in Glenlyon

(105L/1-7, 11-14) and northeast Carmacks (115I/9, 16) areas, central Yukon: Whitehorse, Exploration and Geological Services Division, Yukon Region, Indian and Northern Affairs Canada.

Colpron, M., Mortensen, J. K., Gehrels, G. E., and Villeneuve, M. E., in review-a, Basement complex, Carboniferous magmatic arcs and Paleozoic deformation in Yukon-Tanana Terrane of central Yukon, *in* Colpron, M., Nelson, J. L., and Thompson, R. I., eds., Paleozoic evolution and metallogeny of pericratonic terranes at the ancient Pacific margin of North America, Canadian and Alaskan Cordillera, Geological Association of Canada, p. xxx.

Colpron, M., Murphy, D. C., Nelson, J. L., Roots, C. F., Gladwin, K., Gordey, S. P., Abbott, G., and Lipovsky, P. S., 2002, Preliminary geological map of Glenlyon (105L/1-7, 11-14) and northeast Carmacks (115I/9, 16) areas, Yukon Territory: Geological Survey of Canada, scale 1:125 000.

Colpron, M., Murphy, D. C., Nelson, J. L., Roots, C. F., Gladwin, K., Gordey, S. P., and Abbott, J. G., 2003b, Yukon Targeted Geoscience Initiative: Results of accelerated bedrock mapping in Glenlyon (105L/1-7, 11-14) and northeast Carmacks (115I/9, 16) areas, central Yukon., *in* Emond, D. S., and Lewis, L. L., eds., Yukon Exploration and Geology 2002: Whitehorse, Exploration and Geological Services Division, Yukon Region, Indian and Northern Affairs Canada, p. 85-108.

Colpron, M., Nelson, J. L., Murphy, D. C., Gehrels, G. E., and others, in review-b, A tectonostratigraphic framework for the pericratonic terranes of the northern Cordillera, *in* Colpron, M., Nelson, J. L., and Thompson, R. I., eds., Paleozoic evolution and metallogeny of pericratonic terranes at the ancient Pacific margin of North America, Canadian and Alaskan Cordillera, Geological Association of Canada, p. xxx.

Colpron, M., and Reinecke, M., 2000, Glenlyon Project: Coherent stratigraphic succession from Little Salmon Range (Yukon-Tanana Terrane) and its potential for volcanic-hosted massive sulphide deposits, *in* Emond, D. S., and Weston, L. H., eds., Yukon Exploration and Geology 1999: Whitehorse, Exploration and Geological Services Division, Yukon Region, Indian and Northern Affairs Canada, p. 87-100.

Coney, P. J., Jones, D. L., and Monger, J. W. H., 1980, Cordilleran suspect terranes: Nature, v. 288, no. 27, p. 329-333.

Creaser, R. A., Heaman, L. M., and Erdmer, P., 1997, Timing of high-pressure metamorphism in the Yukon-Tanana terrane, Canadian Cordillera: constraints from U-Pb zircon dating of eclogite from the Teslin tectonic zone: Canadian Journal Earth Sciences, v. 34, p. 709-715.

de Keijzer, M., 2000, Tectonic evolution of the Teslin zone and the western Cassiar terrane, northern Canadian Cordillera [Ph.D. thesis]: University of New Brunswick, 391 p.

de Keijzer, M., Williams, P. F., and Brown, R. L., 1999a, Kilometre-scale folding in the Teslin zone, northern Canadian Cordillera, and its tectonic implications for the accretion of the Yukon-Tanana terrane to North America: Canadian Journal of Earth Sciences, v. 36, p. 479-494.

de Keijzer, M., Williams, P. F., and Carr, S. D., 1999b, Reflections on Lithoprobe-SNORCLE Line 31 in light of the structure of the Teslin zone in the Last Peak area (NTS map 105E/9), southern Yukon Territory, *in* Slave-North American Cordillera Lithospheric Evolution (SNORCLE) Transect and Cordilleran Tectonics Workshop, University of Calgary, p. 114-118.

Enkin, R. J., Johnston, S. T., Larson, K. P., and Baker, J., 2003, Paleomagnetism of the 70 Ma Carmacks volcanics at Solitary Mountain (Yukon) confirms and extends controversial results: Further evidence on the Baja B.C. model, *in* GAC-MAC-SEG Joint Annual Meeting, Vancouver, p. 588.

Erdmer, P., Ghent, E. D., Archibald, D. A., and Stout, M. Z., 1998, Paleozoic and Mesozoic high-pressure metamorphism at the margin of ancestral North America in central Yukon: GSA Bulletin, v. 110, no. 5, p. 615-629.

Fallas, K. M., 1997, Preliminary constraints on the structural and metamorphic evolution of the St. Cyr klippe, south-central Yukon, *in* Slave-North American Cordillera Lithospheric Evolution (SNORCLE) and Cordilleran Tectonics Workshop, p. 90-95.

Ferry, J. M., and Spear, F. S., 1978, Experimental Calibration of the Partitioning of Fe and Mg Between Biotite and Garnet: Contrib. Mineral. Petrol., v. 66, p. 113-117.

Fritz, W. H., Cecile, M. P., Norford, B. S., Morrow, D., and Geldsetzer, H. H. J., 1991, Cambrian to Middle Devonian assemblages, *in* Gabrielse, H., and Yorath, C., eds., Geology of the Cordilleran Orogen in Canada: The Geology of North America, Geological Society of America, p. 151-218.

Ghent, E. D., and Stout, M. Z., 1981, Geobarometry and Geothermometry of Plagioclase-Biotite-Garnet-Muscovite Assemblages: Contrib. Mineral Petrol, v. 76, p. 92-97.

Gladwin, K., Colpron, M., Black, R., and Johnston, S. T., 2003, Bedrock geology at the boundary between Yukon-Tanana and Cassiar terranes, Truitt Creek map area(105L/1), south-central Yukon, *in* Emond, D. S., and Lewis, L. L., eds., Yukon Exploration and Geology 2002: Whitehorse, Exploration and Geological Services Division, Yukon Region, Indian and Northern Affairs Canada, p. 135-148.

Goodfellow, W. D., Cecile, M. P., and Leybourne, M. I., 1995, Geochemistry, petrogenesis, and tectonic setting of lower Paleozoic alkalic and potassic volcanic rocks, northern Canadian Cordilleran miogeocline: Canadian Journal of Earth Sciences, v. 32, no. 8, p. 1236-1254.

Gordey, S. P., and Anderson, R. G., 1993, Evolution of the northern Cordilleran miogeocline, Nahanni map area (105I), Yukon and Northwest Territories: 214, Geological Survey of Canada, 214 p.

Gordey, S. P., and Makepeace, A. J., 2000, Bedrock Geology, Yukon Territory: Exploration and Geological Services Division, Yukon Region, Indian and Northern Affairs Canada, scale 1:1 000 000.

Hansen, V. L., 1992, P-T evolution of the Teslin suture zone Cassiar tectonites, Yukon, Canada: evidence for A- and B- type subduction: Journal of Metamorphic Geology, v. 10, p. 239-263.

Hansen, V. L., Heizler, M. T., and Harrison, M. T., 1991, Mesozoic thermal evolution of the Yukon-Tanana composite terrane : new evidence from $^{40}Ar/^{39}Ar$ data: Tectonics, v. 10, no. 1, p. 51-76.

Harvey, J. L., Carr, S. D., Brown, R. L., and Gallagher, C., 1997, Deformation history and geochronology of plutonic rocks near the d'Abbadie fault, Big Salmon Range, Yukon, *in* Slave-Northern Cordillera Lithospheric Evolution (SNORCLE) and Cordilleran Tectonics Workshop, p. 103-114.

Hunt, P. A., and Roddick, J. C., 1990, A compilation of K-Ar ages: Report 19: Geological Survey of Canada, 3.

Hunt, P. A., and Roddick, J. C., 1991, A compilation of K-Ar ages: Report 20: Geological Survey of Canada, 4.

Hunt, P. A., and Roddick, J. C., 1992, A compilation of K-Ar and ^{40}Ar-^{39}Ar ages: Report 22: Geological Survey of Canada, 6.

Johnston, S. T., 2001, The Great Alaskan Terrane Wreck: Reconciliation of paleomagnetic and geological data in the northern Cordillera: Earth and Planetary Science Letters, v. 193, p. 259-272.

Krogh, T. E., 1982, Improved accuracy of U-Pb zircon ages by the creation of more concordant systems using an air abrasion technique: Geochimica et Cosmochimica Acta, v. 46, p. 637-649.

Meschede, M., 1986, A method of discriminating between different types of mid-ocean ridge basalts and continental tholeiites with the Nb-Zr-Y diagram: Chemical Geology, v. 56, p. 207-218.

Mortensen, J. K., Ghosh, D., and Ferri, F., 1995, U-Pb age constraints of intrusive rocks associated with copper-gold porphyry deposits in the Canadian Cordillera, *in* Shroeder, T. G., ed., Porphyryr deposits of the northwestern Cordillera of North America, Canadian Institute of Mining and Metallurgy, p. 142-158.

Murphy, D. C., Colpron, M., Gordey, S. P., Roots, C. F., Abbott, J. G., and Lipovsky, P. S., 2001, Preliminary bedrock geological map of northern Finlayson Lake area (NTS 105G), Yukon Territory: Exploration and Geological Services Division, Yukon Region, Indian and Northern Affairs Canada, scale 1:100 000.

Murphy, D. C., and Mortensen, J. K., 2003, Late Paleozoic and Mesozoic features constrain displacement on Tintina Fault and limit large-scale orogen-parallel displacement in the Northern Cordillera, *in* GAC-MAC-SEG Joint Annual Meeting, Vancouver, p. 151.

Nelson, J. L., 1993, The Sylvester Allochthon : upper Paleozoic marginal-basin and island-arc terranes in northern British Columbia: Canadian Journal of Earth Sciences, v. 30, p. 631-643.

Nicolas, A., 1995, The Mid-Oceanic Ridges: Mountains Below Sea Level: Berlin, Springer-Verlag, 200 p.

Oliver, D. H., 1996, Structural, kinematic, and thermochronologic studies of the Teslin suture zone, south-central Yukon Territory [Ph.D. thesis]: Southern Methodist University, 231 p.

Pearce, J. A., 1996, A user's guide to basalt discrimination diagrams, Trace element geochemistry of volcanic rocks: applications for massive sulphide exploration: Short Course Notes: St. John's, Geological Association of Canada, p. 79-113.

Pope, M. C., and Sears, J. W., 1997, Cassiar platform, north-central British Columbia: A miogeoclinal fragment from Idaho: Geology, v. 25, p. 515-518.

Roddick, J. A., 1967, Tintina Trench: Journal of Geology, v. 75, p. 23-32.

Roddick, J. C., 1987, Generalized numerical error analysis with application to geochronology and thermodynamics: Geochimica et Cosmochimica Acta, v. 51, p. 2129-2135.

Shervais, 1982, Ti-V plots and the petrogenesis of modern and ophiolitic lavas: Earth and Planetary Science Letters, v. 59, p. 101-118.

Stacey, J. S., and Kramer, J. D., 1975, Approximation of terrestrial lead isotope evolution by a two-stage model: Earth and Planetary Science Letters, v. 26, p. 207-221.

Steiger, R. H., and Jäger, E., 1977, Subcommission on geochronology: convention on the use of decay constants in geo- and cosmochronology: Earth Planetary Science Letters, v. 36, p. 359-362.

Wheeler, J. O., and McFeely, P., 1991, Tectonic assemblage map of the Canadian Cordillera and adjacent parts of the United States of America: Geological Survey of Canada, scale 1:2 000 000.

Winchester, J. A., and Floyd, P. A., 1977, Geochemical discrimination of different magma series and their differentiation products using immobile elements: Chemical Geology, v. 20, no. 4, p. 325-343.

Woodsworth, G. J., Anderson, R. G., and Armstrong, R. L., 1991, Plutonic regimes, Chapter 15, *in* Gabrielse, H., and Yorath, C. J., eds., Geology of the Cordilleran Orogen in Canada: Geology of Canada: Ottawa, Geological Survey of Canada, p. 491-531.

Appendix 2.1: Analytical methods

Electron Microprobe Analyses – University of British Columbia

Analyses were obtained using wavelength dispersive analysis on the University of British Columbia's Cameca SX-50 electron microprobe. The data were collected as oxide percentages, reduced, and used to construct P-T plots using Thermobarometry With Estimation of EQUilibrium state (TWEEQU) software (Berman, 1991). The garnet-biotite thermometer of Berman (1991) and solid solution models of Berman et al. (1995) and Berman and Aranovich (1996) were used. Pressure was determined using the net transfer equilibria reaction for biotite-garnet-muscovite-quartz-aluminosilicate of Ghent and Stoltz (1981) and the solid solution models of Chatterjee and Froese (1975) for mica and Berman et al (1995) and Berman and Aranovich (1996) for garnet and biotite.

ID-TIMS U-Pb Geochronology – University of British Columbia

Zircon was separated from 15-20 kg samples using conventional crushing, grinding, Wilfley table, heavy liquids and Frantz magnetic separator techniques. U-Pb analyses were done using ID-TIMS methods at the Pacific Centre for Isotopic and Geochemical Research at the University of British Columbia. The methodology for zircon grain selection, abrasion, dissolution, geochemical preparation and mass spectrometry are described by Mortensen et al. (1995). All zircon fractions were air abraded (Krogh, 1982) prior to dissolution to minimize the effects of post-crystallization Pb-loss. Procedural blanks for Pb and U were 2 and 1 pg, respectively. Analytical data are listed in Table 2.4 and are plotted on conventional U-Pb concordia diagrams in Figure 2.6. Errors attached to individual analyses were calculated using the numerical error propagation method of

Roddick (1987). Decay constants used are those recommended by Steiger and Jäger (1977). Compositions for initial common Pb were taken from the model of Stacey and Kramer (1975). All errors are given at the 2 sigma level.

Geochemical Analyses – Laurentian University

Samples were prepared using a ceramic mill and analyzed for major, trace and rare-earth elements (REE) at Laurentian University in Sudbury, Ontario. Major element concentrations were determined by fusion X-ray fluorescence (XRF). Trace elements and REE were analyzed by inductively coupled plasma mass spectrometry (ICP-MS) at research detection limits.

CHAPTER 3

Mid-Cretaceous pinning of accreted terranes to miogeoclinal assemblages in the northern Cordillera: Irreconcilable with paleomagnetic data?

Gladwin, Kaesy, School of Earth and Ocean Sciences, University of Victoria, P.O. Box 3055 STN CSC, Victoria, British Columbia V8W 3P6, kaesy@uvic.ca

and

Johnston, Stephen T., School of Earth and Ocean Sciences, University of Victoria, P.O. Box 3055 STN CSC, Victoria, British Columbia V8W 3P6, stj@uvic.ca

Submitted October 6, 2003, to:

Geological Association of Canada Special Volume XX: Paleogeography of the North American Cordillera: Evidence for and against large-scale displacements, J.W. Haggart, R.J. Enkin, and J.W.H. Monger, eds.

3985 words

Corresponding author:

Kaesy Gladwin Phone: (250) 472-4011; Fax: (250) 721-6200
kaesy@uvic.ca

Abstract

This paper reports on geological mapping across the boundary between continental margin assemblages and accreted terranes in the northern Canadian Cordillera. Paleomagnetic data from Late Cretaceous Carmacks Group volcanic rocks that overlie the accreted terranes require 1750 km of post-70 Ma dextral displacement relative to cratonic North America. In the study area, the inboard boundary of the accreted terranes is the Tummel fault zone (TFZ), a 3 km wide northwest-trending belt of 267 Ma greenstone, chert, and harzburgite. Northeast of the TFZ, a Paleozoic continental platform assemblage (Cassiar terrane) includes phyllite, pelitic and psammitic schist, and an upper homogeneous marble unit, and shales out eastward into Selwyn Basin. Southwest of the TFZ, Yukon-Tanana terrane (YTT) consists of Devonian – Mississippian quartzofeldspathic schist and quartzite overlain by Mississippian metasedimentary and metavolcanic rocks, and intruded by two intermediate plutonic suites ca. 340 and 350 Ma. Carmacks Group volcanic rocks unconformably overlie YTT 5 km southeast of the TFZ.

The ~105 Ma Glenlyon Batholith and its satellite plutons intrude Cassiar terrane and the TFZ. Muscovite + biotite + andalusite ± garnet ± cordierite mineral assemblages and margin-parallel schistosity define a contact metamorphic aureole adjacent to the batholith. The aureole extends across the TFZ into YTT, indicating that intrusion postdates terrane amalgamation but predates Carmacks Group volcanics. Two testable explanations are consistent with these observations: (1) Cassiar terrane – Selwyn Basin, previously considered autochthonous, are an east-facing miogeoclinal assemblage exotic to North America; or (2) Late Cretaceous paleomagnetic data do not provide paleolatitude of the accreted terranes.

Introduction

Paleomagnetic data from the northern Cordillera is consistent with large-scale Late Cretaceous dextral translation of the central and western parts of the orogen (e.g. Enkin et al., 2003; Irving and Wynne, 1991; Irving et al., 1996; Wynne et al., 1995). These interpretations conflict, however, with geological mapping which has so far failed to reveal faults along which these displacements could have occurred. Mapped faults can account for only 15 to 20% of the paleomagnetically-determined offsets for Upper Cretaceous layered rocks. This suggests that either the paleomagnetic data are being incorrectly interpreted, or that structures accommodating large amounts of displacement are being systematically overlooked or have not been preserved in the geological record.

Resolving this conflict is fundamental to understanding the links between mountain building and the collision and margin-parallel translation of crustal blocks, as well as the paleogeography and tectonic evolution of much of western North America. If paleomagnetic and geological data cannot be reconciled within a youthful, well-studied orogen, it calls into question the accuracy of plate and paleogeographic reconstructions for Paleozoic and Precambrian time.

This paper describes findings from mapping in Truitt Creek map area (NTS 105L/1; 1:50 000 scale), central Yukon, Canada, which straddles the boundary between the Cassiar and Yukon-Tanana terranes (Fig. 3.1). Yukon-Tanana terrane (YTT) underlies southwestern Yukon (Fig. 3.1A) and is the most inboard of the accreted terranes. YTT is overlain disconformably by Upper Cretaceous volcanic rocks (the Carmacks Group) that yield paleopoles indicating a paleolatitude 1750 ± 550 km south of their current position with respect to cratonic North America (Enkin et al., 2003; Marquis and Globerman,

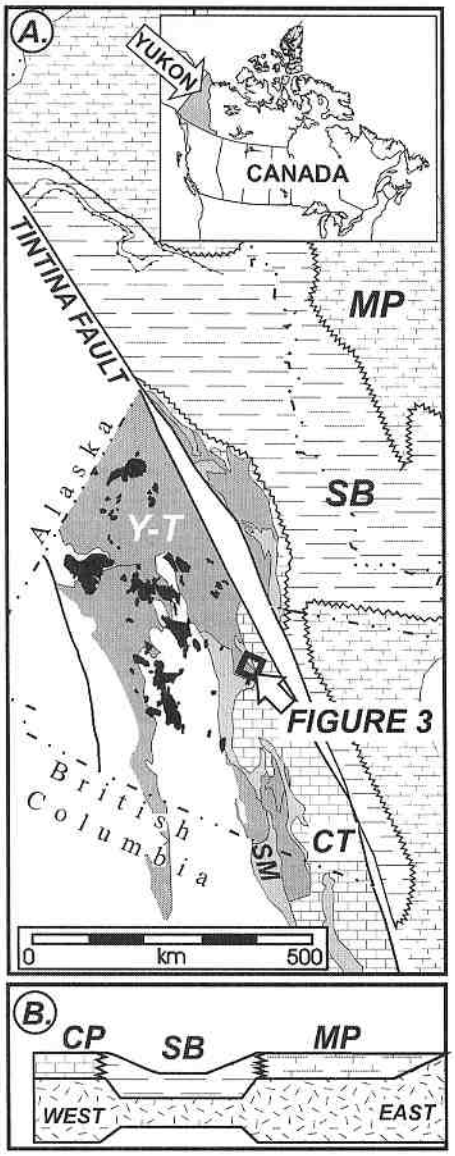

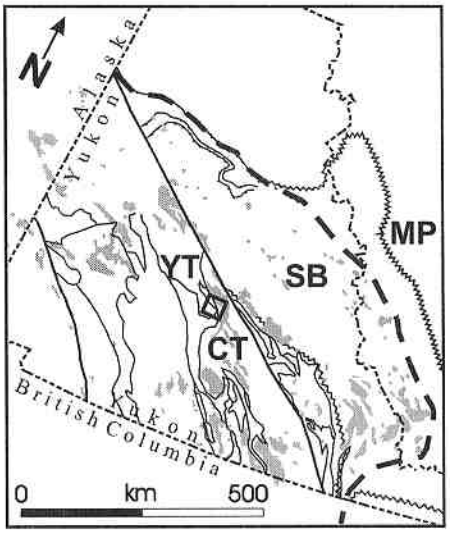

Figure 3.1 (left): A. Geographic distribution of Cassiar (CT), Yukon-Tanana (Y-T), and Slide Mountain (SM) terranes, Selwyn Basin (SB), and Mackenzie Platform (MP), with 425 km of dextral strike-slip motion restored on Tintina fault system (modified after Wheeler and McFeely, 1991). Distribution of 70 Ma Carmacks Group volcanic rocks is shown in black (modified after Wynne et al., 1998). B. Schematic cross-sectional representation of Cassiar platform (CP) and Selwyn Basin with respect to Mackenzie platform.

Figure 3.2 (right): Map of Yukon Territory showing regional distribution of mid-Cretaceous intrusions (shaded areas); thick dashed line indicates eastern extent of magmatism (modified after Woodsworth et al., 1991). Box shows location of study area in Figure 3.3.

1988; Wynne et al., 1998). Cassiar terrane in Yukon is characterized by a platformal carbonate sequence and has been considered as parautochthonous (e.g. Gabrielse et al., 1991) or displaced (Pope and Sears, 1997) ancient North American margin.

We address the question, "Is the boundary between accreted terranes and platformal rocks of North American affinity a Late Cretaceous structure that has accommodated >1000 km of dextral strike-slip displacement?"

Tectonic elements in central Yukon

Cassiar terrane is a ~1500 km long northwest-trending Late Precambrian - Paleozoic miogeoclinal assemblage (Wheeler and McFeely, 1991). Two units characterize the terrane in the study area: the Cambrian-Ordovician Kechika Group, a clastic succession capped by intercalated sandstone and limestone, and the overlying Silurian-Devonian Askin Group, a graphitic carbonate succession. Cassiar platform facies shales out to the east into the Selwyn Basin, a region underlain by deep marine shale-dominated stratigraphy (Gordey and Anderson, 1993). Cassiar platform – Selwyn Basin define an east-facing continental margin interpreted as a Late Silurian – Middle Devonian offshore basement high that was an integral part of the ancient North American miogeocline, perhaps analogous to Bahamas on the modern North Atlantic passive margin.

West of Cassiar Terrane, YTT is a northwest-trending polydeformed and metamorphosed pericratonic terrane consisting of Devonian – Mississippian quartzofeldspathic sedimentary rocks and Mississippian – Pennsylvanian continental arc successions (Colpron et al., in review; Mortensen, 1992).

Latest Devonian to Permian oceanic rocks referred to as Slide Mountain terrane (Monger, 1993; Plint and Gordon, 1997) occur as allochthonous sheets that structurally overlie YTT and are also thrust eastward onto Cassiar terrane (Gabrielse, 1991; Gordey and Makepeace, 2000).

Mid-Cretaceous intrusions are widespread (Fig. 3.2). An outboard belt along the west coast characterised by I-type magmatism contrasts with a coeval belt ~1000 km inboard of predominantly S-type granitoids (e.g. Monger et al., 1982). The Omineca-Selwyn plutonic belt in Yukon is part of the inboard magmatic front (Monger et al., 1982; Wheeler and McFeely, 1991).

Solitary Mountain

At Solitary Mountain, immediately south of the study area, the easternmost lava flows of the 70 Ma Carmacks Group unconformably overlie YTT rocks continuous with those mapped in Truitt Creek map area. A primary magnetic remanence is statistically indistinguishable from that determined from Carmacks Group volcanic rocks studied to the west, and requires 1750 ± 550 km of post-70 Ma northward displacement (Enkin et al., 2003; Wynne et al., 1998). Two major geological structures separate Solitary Mountain from the North American craton – the Tintina and Tummel fault zones, located 25 and 5 km to the northeast, respectively.

Geological evolution recorded in Truitt Creek map area

Truitt Creek map area is 25 km southwest of the northwest-striking Tintina Trench fault, an Eocene dextral strike-slip fault with 425 km displacement (Fig. 1A; Murphy and Mortensen, 2003; Roddick, 1967), and is bisected by the northwest-striking Tummel fault zone (TFZ; Fig. 3.3). Along strike to the north, the Tummel fault is truncated by the Big Salmon fault (Colpron et al., 2002).

Northeast of the TFZ, two units are recognized in a miogeoclinal sedimentary succession (Fig. 3.3). The >300 m thick lower unit (Unit 1) is dominantly massive, black, locally calcareous phyllite, with 10 cm to 2-3 m intercalated sandstone and limestone layers near its top. Conformably overlying Unit 1 is >100 m of a massive, light grey to black, locally graphitic marble unit (Unit 2).

Chlorite and muscovite are common and indicate low-grade regional metamorphism. Structural fabrics and metamorphic assemblages are overprinted in a contact aureole imposed by Glenlyon Batholith (discussed below). Units 1 and 2 are older than the mid-Cretaceous Glenlyon Batholith; poorly preserved conodonts from Unit 2 suggest a Paleozoic age (M.J. Orchard *in* Gladwin et al., Chapter 2). Based on similar lithology and stratigraphy, we correlate Units 1 & 2 with the Kechika and Askin groups, respectively, which occur south of and are also intruded by Glenlyon Batholith, consistent with inclusion of these rocks in Cassiar terrane.

Southwest of the TFZ is a Paleozoic succession of foliated siliciclastic, volcaniclastic, and volcanic rocks, intruded by 348-349 Ma quartz diorite and granodiorite. Mafic to intermediate metavolcanic and metavolcaniclastic rocks, chlorite schist,

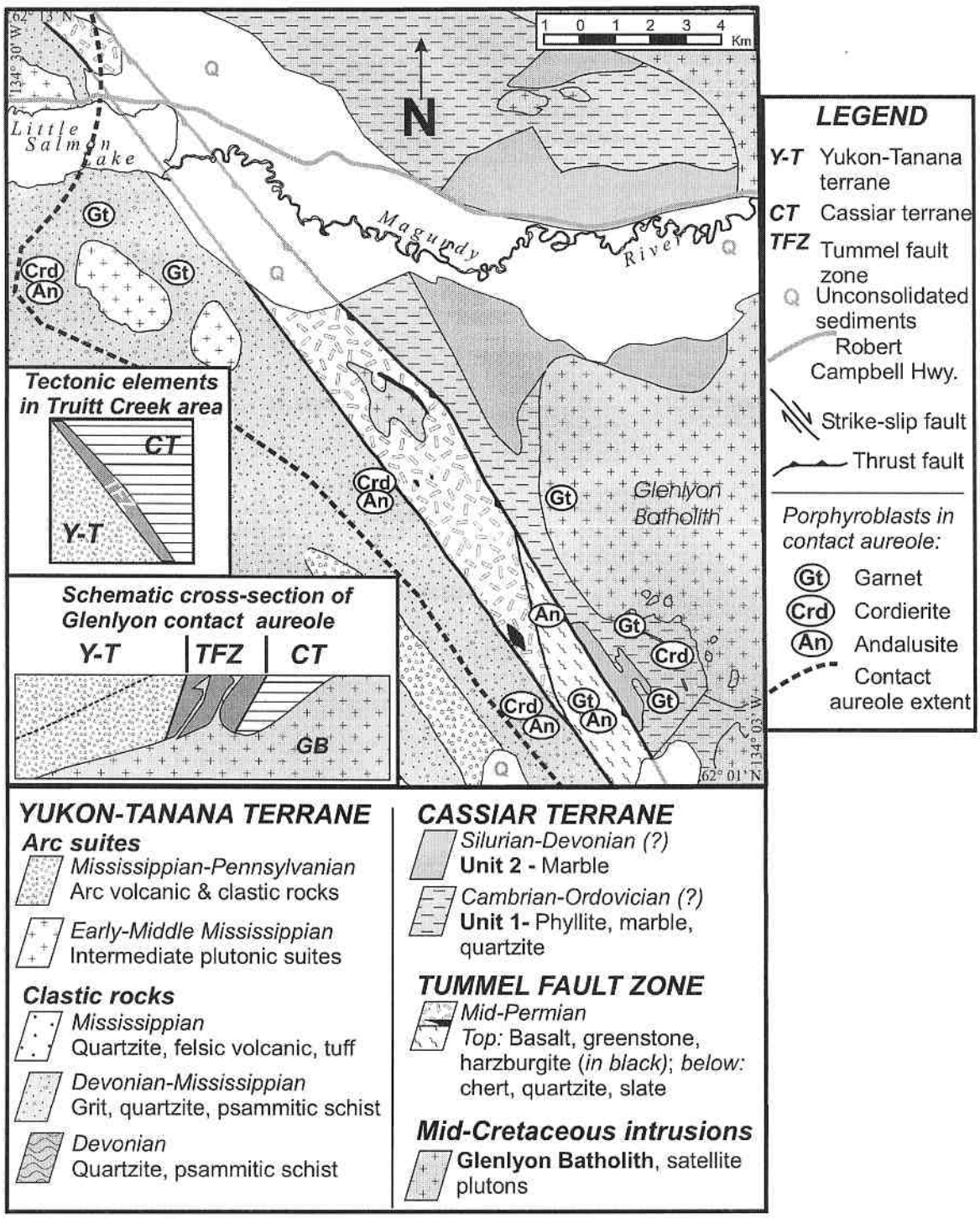

Figure 3.3: Bedrock geology of Truitt Creek map area. Tectonic element diagram (inset) modified after Gordey and Makepeace (2000).

metaconglomerate, and marble overlies the lower clastic-dominated succession. A ca. 340 Ma U-Pb zircon age from basal quartz-feldspar porphyry provides a maximum age for this succession (Colpron et al., in review). Ar-Ar mica cooling ages of 180-190 Ma constrain fabric development and metamorphism to pre-mid-Jurassic time (Oliver, 1996).

Based on similar lithology, age, and tectonostratigraphy, we include these rocks in YTT, consistent with this succession being continuous with mapped YTT to the northwest (Colpron et al., 2002) and to the south (Tempelman-Kluit, 1984).

Foliated greenstone, serpentinized harzburgite, chert and argillite occur within the 1-3 km wide TFZ (Fig. 3.3). Widespread epidote and chlorite indicate middle greenschist facies metamorphic conditions. A sample of greenstone yielded a preliminary U-Pb zircon age of 267 Ma (Chapter 2). Similar lithologies and age suggests correlation of TFZ rocks with the Slide Mountain terrane (Colpron et al., 2003).

The TFZ has a complex deformational history, with late brittle structures that overprint several generations of earlier ductile deformation. Age of deformation is constrained to be post-mid-Permian (the age of basalt deformed within the zone) but syn- or pre-mid-Cretaceous (the age of undeformed plutons within the zone which are syn- to post-tectonic).

Glenlyon Batholith: A mid-Cretaceous pin

Glenlyon Batholith is an 80 km long multi-phase intrusion of the Omineca-Selwyn plutonic belt (Woodsworth et al., 1991). It dominates the eastern part of the study area, where it intrudes Unit 1 (Fig. 3.3). Hornblende granodiorite was succeeded by a

voluminous biotite ± muscovite granite, with rare late-stage muscovite-plagioclase pegmatite dykes. Oriented hornblende and plagioclase phenocrysts locally define a weak magmatic foliation. Pendants and xenoliths of metapelitic country rock metamorphosed to lower amphibolite grade are common. Gently to moderately (~30°) southwest-dipping 5-15 m thick sills separated by 1-3 m thick country rock septa were observed in some exposures, suggesting an overall southwest-dipping sheet-like geometry of the intrusive body.

Plutons and dykes of hornblende leucogabbro and hornblende diorite within the Tummel fault zone are an early mafic phase of Glenlyon magmatism. Alignment of magmatic mafic minerals defines a magmatic foliation. Plagioclase crystals with distinct sericite-altered cores are similar to crystals noted in the hornblende granodiorite phase of the batholith.

Leucogabbro intruding the TFZ yielded a U-Pb zircon age of ~105 Ma (Chapter 2). Hornfels from northeastern Truitt Creek map area yielded a whole-rock K-Ar cooling age of 105 ± 4 Ma (Hunt and Roddick, 1990). Correlation with the d'Abbadie pluton, 15 km along strike to the south, which has yielded a U-Pb monazite age of 109 ± 3 Ma (de Keijzer, 2000), and with a porphyry at Clear Lake, 70 km along strike to the northwest, which has yielded a ca. 108 Ma U-Pb zircon age (Breitsprecher et al., 2002), supports a similar age for the Glenlyon intrusion.

A high-temperature, low- to moderate pressure greenschist to amphibolite grade contact aureole post-dates and overprints regionally developed metamorphic assemblages in parts of YTT, Cassiar terrane, and the TFZ. Near the margin, the contact aureole is characterized by a well-developed margin-parallel schistosity reminiscent of regionally

metamorphosed rocks. About 2-3 km beyond the intrusive margin, schistosity is not developed, and metamorphic grade decreases. Diagnostic mineral assemblages include biotite + muscovite ± cordierite ± andalusite ± garnet in metapelites. In map view, the aureole extends 5-10 km southwest from the exposed margin of the main batholith; the shallow southwest dip inferred for the batholith suggests a structural thickness for the aureole of ~3 km (Fig. 3.3, inset) because the contact aureole encompasses parts of the TFZ, YTT, and Cassiar terrane (Fig. 3.3). The mid-Cretaceous emplacement of Glenlyon Batholith and its satellite intrusions in the TFZ post-dates and provides a minimum age constraint for the assembly of Yukon-Tanana, Slide Mountain, and Cassiar terranes.

Discussion

Geological relationships established in the Truitt Creek map area indicate that by the 70 Ma eruption of the Carmacks Group, YTT and Cassiar terrane were pinned to one another; the mid-Cretaceous Glenlyon Batholith and its satellite plutons intrude Cassiar terrane and the TFZ, and the related contact aureole extends from Cassiar terrane well into YTT. The 1750 ± 550 km of dextral translation required by Carmacks Group paleomagnetic data must therefore apply not only to YTT, but to Cassiar terrane as well. About 425 km of displacement can be accounted for along the Tintina fault (Murphy and Mortensen, 2003), leaving some 1325 ± 550 km unaccounted for.

The mid-Cretaceous Omineca-Selwyn plutonic belt pins together Cassiar terrane and Selwyn Basin (Fig. 2; Wheeler and McFeely, 1991; Woodsworth et al., 1991). Thus, if the paleomagnetic data are accepted, a tectonic entity encompassing this platform-to-

basin margin that has long been considered to be of North American affinity, must also be far-travelled. This would require >1300 ± 550 km of dextral displacement along or within the Mackenzie platformal succession east of Selwyn Basin.

Two interpretations of these new constraints are offered:

1. By showing that the paleomagnetic data must be applied to a large area of continental margin assemblages of North American affinity, we have demonstrated that the paleomagnetic data must NOT be providing an accurate assessment of paleolatitude for Upper Cretaceous Cordilleran rocks.

2. The east-facing Cassiar platform – Selwyn basin continental margin must be far-travelled and exotic with respect to North America.

Recently published detrital zircon and paleomagnetic studies are consistent with interpretation of the paleomagnetic data as being in error. Detrital zircons from Late Cretaceous basins within the western Cordillera are interpreted by Mahoney et al. (1999) to demonstrate a North American cratonic source that would preclude significant post-depostional northward translation, although Housen and Beck (1999) reinterpreted these data as being consistent with such motion. One study used data from plutons of similar age and in the same terrane belt as Glenlyon batholith in the southernmost Canadian Cordillera to show no significant displacement relative to North America (Irving and Archibald, 1990). However, it is difficult to assess paleohorizontal for plutons, and this adds uncertainty to paleomagnetic studies of plutonic rocks. Some paleomagnetic studies (Enkin et al., 2003; Mahoney et al., 2003) have suggested rates of northward translation

approaching the plate tectonic speed limit, as well as an interval of mid-Cretaceous southward translation of much of the Cordillera.

Rejecting the paleomagnetic data is, however, difficult to reconcile with the number of consistent studies, or with the successful application of paleomagnetic techniques for Late Cretaceous rocks elsewhere. Alternative explanations such as experimental or dating errors, anomalous geomagnetic behaviour, or systematic re-orientation of Cordilleran paleomagnetic data by structural or hydrothermal means are inadequate or improbable (e.g. Beck, 1991). While it is beyond the scope of this paper to investigate processes that may have resulted in systematically erroneous paleomagnetic results, should we ever reach a stage where it becomes certain that it is the paleomagnetic data which are in error, a concerted research effort would be required to explain such a phenomenon.

Interpretation of the Cassiar platform and Selwyn basin as an east-facing continental margin is consistent with the presence of east-facing continental margin assemblages along the inboard portion of much of the Cordillera. These include the Nixon Fork platform to Dillinger basin in Alaska and the Caribou platform to Ishbel basin in the southern Canadian Cordillera (Johnston, 2001). Regional and detailed geological mapping has, however, not resulted in recognition of structures or stratigraphy that could accommodate the Late Cretaceous translation of this exotic margin. Mid-Cretaceous foreland basin formation and westerly derived sedimentation on North America casts further doubt on interpretations that require an intervening basin between the east-facing Cassiar – Selwyn continental margin assemblage and the North American craton.

Several workers have suggested that preservation and/or recognition of strike-slip faults that record large-scale lateral displacements is unlikely, and that paleomagnetism

may in fact be the only reliable indicator of paleogeography in translated terranes (e.g. Umhoefer, 2000; Woodcock, 1986). Reasons for this include: post-translation destruction, reactivation, or covering of such faults; distribution of large amounts of translation over many anastomosing faults, each recording much smaller displacement; and low preservation potential of fault evidence in some rocks, such as oceanic crust, that undergo post-translation accretionary events. Thus, paleomagnetic and geologic data would remain irreconcilable.

Neither of our suggested interpretations is without problems. Both hypotheses are, however, testable. Paleomagnetic studies of Cretaceous volcanic rocks overlying Selwyn basin stratigraphy, or of coeval Selwyn basin and Mackenzie platform strata, should aid in constraining the paleogeographic evolution of the Northern Cordillera. Detailed structural and stratigraphic studies across the eastern margin of the Omineca Belt should also prove instructive.

Conclusions

A. A Paleozoic miogeoclinal sequence assigned to Cassiar terrane, and a Paleozoic clastic and arc succession assigned to YTT are juxtaposed along the TFZ in central Yukon Territory.

B. The mid-Cretaceous Glenlyon Batholith and its contact aureole extends across the TFZ, pinning YTT to Cassiar terrane by ca. 105 Ma. Related coeval plutons also pin Cassiar terrane to Selwyn Basin at this time.

C. Paleomagnetic interpretations from 70 Ma volcanic rocks overlying YTT require ~1750 km of dextral strike-slip displacement since eruption. Only ~425 km of northward translation can be accommodated by known structures. Either the paleomagnetic data are not providing paleolatitude, or Cassiar terrane and Selwyn Basin as well as the terranes to the west are far-travelled.

Acknowledgements

This research was supported by an NSERC Discovery Grant to STJ, research grants and field support by the Yukon Geological Survey, and by logistical support provided by Randy Enkin of the Geological Survey of Canada. The authors thank Maurice Colpron, Bernie Housen and Paul Umhoefer for thoughtful reviews of the manuscript; Robin Black (Acadia University), Maurice Colpron (Yukon Geological Survey) and Randy Enkin (Geological Survey of Canada) for discussions and assistance in the field; Jim Mortensen (University of British Columbia) for geochronological data; and Dante Canil and Joe English (University of Victoria) for discussion.

References

Beck, M. E., Jr., 1991, Case for northward transport of Baja and coastal southern California: Paleomagnetic data, analysis, and alternatives: Geology, v. 19, p. 506-509.

Breitsprecher, K., Mortensen, J. K., and Villeneuve, M. E., 2002, YukonAge 2002: A database of isotopic age determinations for rock units from Yukon Territory, Canada, Exploration and Geological Services Division, Yukon Region, Indian and Northern Affairs Canada.

Colpron, M., Mortensen, J. K., Gehrels, G. E., and Villeneuve, M. E., in review, Basement complex, Carboniferous magmatic arcs and Paleozoic deformation in Yukon-Tanana Terrane of central Yukon, *in* Colpron, M., Nelson, J. L., and Thompson, R. I., eds., Paleozoic evolution and metallogeny of pericratonic terranes at the ancient Pacific margin of North America, Canadian and Alaskan Cordillera, Geological Association of Canada, p. xxx.

Colpron, M., Murphy, D. C., Nelson, J. L., Roots, C. F., Gladwin, K., Gordey, S. P., Abbott, G., and Lipovsky, P. S., 2002, Preliminary geological map of Glenlyon (105L/1-7, 11-14) and northeast Carmacks (115I/9, 16) areas, Yukon Territory: Geological Survey of Canada, scale 1:125 000.

Colpron, M., Murphy, D. C., Nelson, J. L., Roots, C. F., Gladwin, K., Gordey, S. P., and Abbott, J. G., 2003, Yukon Targeted Geoscience Initiative: Results of accelerated bedrock mapping in Glenlyon (105L/1-7, 11-14) and northeast Carmacks (115I/9, 16) areas, central Yukon., *in* Emond, D. S., and Lewis, L. L., eds., Yukon Exploration and Geology 2002: Whitehorse, Exploration and Geological Services Division, Yukon Region, Indian and Northern Affairs Canada, p. 85-108.

de Keijzer, M., 2000, Tectonic evolution of the Teslin zone and the western Cassiar terrane, northern Canadian Cordillera [Ph.D. thesis]: University of New Brunswick, 391 p.

Enkin, R. J., Johnston, S. T., Larson, K. P., and Baker, J., 2003, Paleomagnetism of the 70 Ma Carmacks volcanics at Solitary Mountain (Yukon) confirms and extends

controversial results: Further evidence on the Baja B.C. model, *in* GAC-MAC-SEG Joint Annual Meeting, Vancouver, p. 588.

Gabrielse, H., 1991, Late Paleozoic and Mesozoic terrane interactions in north-central British Columbia: Canadian Journal of Earth Sciences, v. 28, p. 947-957.

Gabrielse, H., Monger, J. W. H., Wheeler, J. O., and Yorath, C. J., 1991, Chapter 2, Tectonic Framework, Part A. Morphological belts, tectonic assemblages and terranes, *in* Gabrielse, H., and Yorath, C. J., eds., Geology of the Cordilleran Orogen in Canada: Denver, Colorado, Geological Society of America, p. 15-28.

Gordey, S. P., and Anderson, R. G., 1993, Evolution of the northern Cordilleran miogeocline, Nahanni map area (105I), Yukon and Northwest Territories: 214, Geological Survey of Canada, 214 p.

Gordey, S. P., and Makepeace, A. J., 2000, Bedrock Geology, Yukon Territory: Exploration and Geological Services Division, Yukon Region, Indian and Northern Affairs Canada, scale 1:1 000 000.

Housen, B., and Beck, M. E., Jr., 1999, Testing terrane transport: An inclusive approach to the Baja B.C. controversy: Geology, v. 27, no. 12, p. 1143-1146.

Hunt, P. A., and Roddick, J. C., 1990, A compilation of K-Ar ages: Report 19: Geological Survey of Canada, 3.

Irving, E., and Archibald, D. A., 1990, Bathozonal tilt corrections to paleomagnetic data from Mid-Cretaceous plutonic rocks: Examples from the Omineca Belt, British Columbia: Journal of Geophysical Research, v. 95, no. B4, p. 4579-4585.

Irving, E., and Wynne, P. J., 1991, Chapter 3, Paleomagnetism: Review and Tectonic Implications, *in* Gabrielse, H., and Yorath, C. J., eds., Geology of the Cordilleran Orogen in Canada: Denver, Colorado, Geological Society of America, p. 61-86.

Irving, E., Wynne, P. J., Thorkelson, D. J., and Schiarizza, P., 1996, Large (1000 - 4000 km) northward movements of tectonic domains in the northern Cordillera, 83 to 45 Ma: Journal of Geophysical Research, v. 101, p. 17901-17916.

Johnston, S. T., 2001, The Great Alaskan Terrane Wreck: Reconciliation of Paleomagnetic and Geological Data in the northern Cordillera: Earth and Planetary Science Letters, v. 193, p. 259-272.

Mahoney, J. B., Link, P. K., Riesterer, J. K., Enkin, R. J., and Haskin, M. L., 2003, The paleogeographic significance of the Silverquick/Powell Creek Succession, south-central

British Columbia, *in* GAC-MAC-SEG Joint Annual Meeting, Vancouver, p. 754.

Mahoney, J. B., Mustard, P. S., Haggart, J. W., Friedman, R. M., Fanning, C. M., and McNicoll, V. J., 1999, Archean zircons in Cretaceous strata of the western Canadian Cordillera: The "Baja B.C." hypothesis fails a "crucial test": Geology, v. 27, p. 195-198.

Marquis, G., and Globerman, B. R., 1988, Northward motion of the Whitehorse Trough: paleomagnetic evidence from the Upper Cretaceous Carmacks Group: Canadian Journal of Earth Sciences, v. 25, p. 2005-2016.

Monger, J. W. H., 1993, Cretaceous tectonics of the North American Cordillera, *in* Caldwell, W. G. E., and Kauffman, E. G., eds., Evolution of the Western Interior Basin: Special Paper, Geological Association of Canada, p. 31-47.

Monger, J. W. H., Price, R. A., and Tempelman-Kluit, D. J., 1982, Tectonic accretion and the origin of the two major metamorphic and plutonic welts in the Canadian Cordillera: Geology, v. 10, p. 70-75.

Mortensen, J. K., 1992, Pre-mid-Mesozic tectonic evolution of the Yukon-Tanana Terrane, Yukon and Alaska: Tectonics, v. 11, no. 4, p. 836-853.

Murphy, D. C., and Mortensen, J. K., 2003, Late Paleozoic and Mesozoic features constrain displacement on Tintina Fault and limit large-scale orogen-parallel displacement in the Northern Cordillera, *in* GAC-MAC-SEG Joint Annual Meeting, Vancouver, p. 151.

Oliver, D. H., 1996, Structural, kinematic, and thermochronologic studies of the Teslin suture zone, south-central Yukon Territory [Ph.D. thesis]: Southern Methodist University, 231 p.

Plint, H. E., and Gordon, T. M., 1997, The Slide Mountain terrane and the structural evolution of the Finlayson Lake fault zone, southeastern Yuko: Canadian Journal of Earth Sciences, v. 34, p. 105-126.

Pope, M. C., and Sears, J. W., 1997, Cassiar platform, north-central British Columbia: A miogeoclinal fragment from Idaho: Geology, v. 25, p. 515-518.

Roddick, J. A., 1967, Tintina Trench: Journal of Geology, v. 75, p. 23-32.

Tempelman-Kluit, D. J., 1984, Geology, Laberge (105E) and Carmacks (105I), Yukon Territory: Geological Survey of Canada, scale 1:250 000.

Umhoefer, P. J., 2000, Where are the missing faults in translated terranes?: Tectonophysics, v. 326, p. 23-35.

Wheeler, J. O., and McFeely, P., 1991, Tectonic assemblage map of the Canadian Cordillera and adjacent parts of the United States of America: Geological Survey of Canada, scale 1:2 000 000.

Woodcock, N. H., 1986, The role of strike-slip fault systems at plate boundaries: Philosophical Transactions of the Royal Society of London, v. 317, p. 13-29.

Woodsworth, G. J., Anderson, R. G., and Armstrong, R. L., 1991, Plutonic regimes, Chapter 15, *in* Gabrielse, H., and Yorath, C. J., eds., Geology of the Cordilleran Orogen in Canada: Geology of Canada: Ottawa, Geological Survey of Canada, p. 491-531.

Wynne, P. J., Enkin, R. J., Baker, J., Johnston, S. T., and Hart, C. J. R., 1998, The Big Flush - Paleomagnetic signature of a 70 Ma regional hydrothermal event in displaced rocks of the northern Canadian Cordillera: Canadian Journal of Earth Sciences, v. 35, p. 657-671.

Wynne, P. J., Irving, E., Maxson, J. A., and Kleinspehn, K. L., 1995, Paleomagnetism of the Upper Cretaceous strata of Mount Tatlow: Evidence for 3000 km of northward displacement of the eastern Coast Belt, British Columbia: Journal of Geophysical Research, v. 100, no. B4, p. 6073-6091.

CHAPTER 4

Conclusions

Contributions of the study

Two principal contributions have been made by this study.

(1) Stratigraphy has been established within Truitt Creek map area, and correlated with units recognized regionally. Paleozoic miogeoclinal assemblages in the northeast (Kechika and Askin groups) of Cassiar terrane contrast with metaclastic and metaigneous rocks in Yukon-Tanana terrane to the southwest.

(2) Mid-Cretaceous Glenlyon Batholith and its satellite intrusions occur in Cassiar terrane and the Tummel fault zone, and contact metamorphism attributable to these intrusions is recognized in Cassiar terrane, the Tummel fault zone, and into Yukon-Tanana terrane. Thus, these three tectonic entities were in approximately their present configuration relative to one another prior to ca. 105 Ma (the age of the intrusions). An implication of this is that the Tummel fault zone cannot have accommodated large-scale displacement required by paleomagnetic data from nearby Solitary Mountain.